

# Mathematical Modeling of SISO based Timoshenko Structures – A Case Study

T.C. Manjunath, *Student Member IEEE*, and B. Bandyopadhyay, *Member IEEE*

**Abstract**—This paper features the mathematical modeling of a single input single output based Timoshenko smart beam. Further, this mathematical model is used to design a multirate output feedback based discrete sliding mode controller using Bartoszewicz law to suppress the flexural vibrations. The first 2 dominant vibratory modes is retained. Here, an application of the discrete sliding mode control in smart systems is presented. The algorithm uses a fast output sampling based sliding mode control strategy that would avoid the use of switching in the control input and hence avoids chattering. This method does not need the measurement of the system states for feedback as it makes use of only the output samples for designing the controller. Thus, this methodology is more practical and easy to implement.

**Keywords**—Smart structure, Timoshenko beam theory, Discrete sliding mode control, Bartoszewicz law, Finite Element Method, State space model, Vibration control, Mathematical model, SISO.

## I. INTRODUCTION

MATHEMATICAL modeling of any system is the art and craft of building a system of equations that is both sufficiently complex and simple to give real insight into the situation. It brings together mathematicians and specialists in other fields to improve existing system, develop better ones, or predict the behavior of a certain system and how the things will be in the future. With the advent of more powerful computers, modeling teams have been able to tackle more complex problems, develop more accurate models, get answers in less time, and reduce research and development costs. Finally, it is the process of creating a mathematical representation of some phenomenon in order to gain a better understanding of that phenomenon.

It is a process that attempts to match observation with symbolic statement. During the process of building a mathematical model, the modeler will decide what factors are relevant to the problem and what factors can be de-emphasized. Once a model has been developed and used to answer questions, it should be critically examined and often

T.C. Manjunath is a Research Scholar in the Interdisciplinary Programme in Systems and Control Engineering, Indian Institute of Technology Bombay, Powai, Mumbai-400076, Maharashtra, India. (Corresponding author's phone : +91 22 25767884; fax: +91 22 25720057; e-mail: [temanju@sc.iitb.ac.in](mailto:temanju@sc.iitb.ac.in), [temanjunath@gmail.com](mailto:temanjunath@gmail.com), URL : <http://www.sc.iitb.ac.in/~tcmmanju>).

Dr. Bijnan Bandyopadhyay is with the Interdisciplinary Programme in Systems and Control Engineering, Indian Institute of Technology Bombay, IIT Bombay, Mumbai-76, Maharashtra, India and is currently in the Professor cadre.

modified to obtain a more accurate reflection of the observed reality of that phenomenon. Mathematical models of time dependent processes (dynamical systems) can be split into 2 categories depending on how the time variable is to be treated. A continuous-in-time mathematical model is based on a set of equations that are valid for any value of the time variable. A discrete-in-time mathematical model is designed to provide information about the state of the physical system only at a selected set of distinct times.

The solution of a continuous-in-time mathematical model provides information about the physical phenomenon at every time value. The solution of a discrete-in-time mathematical model provides information about the physical system at only a finite number of time values. Continuous-in-time models have 2 advantages over discrete-in-time models - they provide information at all times and more clearly show the qualitative effects that can be expected when a parameter or an input variable is changed. On the other hand, discrete in time models have 2 advantages over continuous in time models - they are less demanding with respect to skill level in algebra, trigonometry, calculus, differential equations, etc. and are better suited for digital implementation on a computer.

The main advantage of mathematical modeling of systems (say, a structure) is simulating the system off-line, observing its behavioral response and then using it to control in real time. For the control of these structures, a precise mathematical model is required to start with. These mathematical models are further used to design a controller and put it in the feedback loop with the plant for its overall satisfactory performance. It is common to assume the availability of a model of the plant to be controlled, especially in the form of a differential equation or a system of differential equations (i.e., an input-output relation or the state space model). The number of inputs and outputs or the number of states of a system can be regarded as parameters that are used to control the system. This approach work well for mechanical systems with a few DOF, keeping in mind that each DOF gives rise to 2 state variables, viz., displacement and velocity. A structural dynamic model or a finite element model is obtained by the finite element discretization of a structure and then using the modern control theory, a state-space model of the structural system can be obtained.

Many researchers have developed mathematical models of flexible structures and used them for controlling various parameters, say the transverse vibrations of the system when the structure is subjected to external disturbances. The

following paragraphs give a brief insight into such mathematical models and its control designs for damping out the vibrations.

Culshaw [15] discussed the concept of smart structure, its benefits and applications. Rao and Sunar [35] explained the use of piezo materials as sensors and actuators in sensing vibrations in a survey paper. Baily and Hubbard [7] have studied the application of piezoelectric materials as sensor / actuator for flexible structures. Hanagud *et.al.* [26] developed a Finite Element Model (FEM) for a beam with many distributed piezoceramic sensors / actuators. Fanson *et.al.* [21] performed some experiments on a beam with piezoelectrics using positive position feedback. Balas [8] did extensive work on the feedback control of flexible structures. Experimental evaluation of piezoelectric actuation for the control of vibrations in a cantilever beam was presented by Burdett *et.al.* [9]. Brenan *et.al.* [10] performed some experiments on the beam for different actuator technologies. Yang and Lee [49] studied the optimization of feedback gain in control system design for structures. Crawley and Luis [13] presented the development of piezoelectric sensor / actuator as elements of intelligent structures.

Hwang and Park [27] presented a new finite element (FE) modeling technique for flexible beams. Continuous time and discrete time algorithms were proposed to control a thin piezoelectric structure by Bona, *et.al.* [11]. Schiehlen and Schonstedt [38] reported the optimal control designs for the first few vibration modes of a cantilever beam using piezoelectric sensors / actuators. S.B. Choi *et.al.* [17] have shown a design of position tracking sliding mode control for a smart structure. Distributed controllers for flexible structures can be seen in Forouza Pourki [22]. Shiang Lee [40] devised a new form of control strategy for vibration control of smart structures using neural networks. A passivity-based control for smart structures was designed by Gosavi and Kelkar [24]. A self tuning active vibration control scheme in flexible beam structures was carried out by Tokhi [42]. Active control of adaptive laminated structures with bonded piezoelectric sensors and actuators was investigated by Moita *et.al.* [32]. Ulrich *et.al.* [44] devised a optimal LQG control scheme to suppress the vibrations of a cantilever beam. Finite element simulation of smart structures using an optimal output feedback controller for vibration and noise control was performed by Young *et.al.* [48]. Work on vibration suppression of flexible beams with bonded piezo-transducers using wave-absorbing controllers was done by Vukowich and Koma [45].

Aldraihem *et.al.* [2] have developed a laminated beam model using two theories; namely, Euler-Bernoulli beam theory and Timoshenko Beam theory. Abramovich [3] has presented analytical formulation and closed form solutions of composite beams with piezoelectric actuators, which was based on Timoshenko beam theory. He also studied the effects of actuator location and number of patches on the actuator's performance for various configurations of the piezo patches and boundary conditions under mechanical and / or

electric loads. Using a higher-order shear deformation theory, Chandrashekhara and Varadarajan [14] presented a finite element model of a composite beam to produce a desired deflection in beams with clamped-free, clamped-clamped and simply supported ends.

Sun and Zhang [36] suggested the idea of exploiting the shear mode to create transverse deflection in sandwich structures. Here, he proved that embedded shear actuators offer many advantages over surface mounted extension actuators. Aldraihem and Khdeir [4] proposed analytical models and exact solutions for beams with shear and extension piezoelectric actuators and the models were based on Timoshenko beam theory and higher-order beam theory. Exact solutions were obtained by using the state-space approach. Doschner and Enzmann [19] designed a model-based controller for smart structures. Robust multivariable control of a double beam cantilever smart structure was implemented by Robin Scott *et.al.* [33].

In a more recent work, Zhang and Sun [51] formulated an analytical model of a sandwich beam with shear piezoelectric actuator that occupies the entire core. The model derivation was simplified by assuming that the face layers follow Euler-Bernoulli beam theory, whereas the core layer obeys Timoshenko beam theory. Furthermore, a closed form solution of the static deflection was presented for a cantilever beam. A new method of modeling and shape control of composite beams with embedded piezoelectric actuators was proposed by Donthireddy and Chandrashekhara [20].

A model reference method of controlling the vibrations in flexible smart structures was shown by Murali *et.al.* [31]. Thomas and Abbas [41] explained some techniques of performing finite element methods for dynamic analysis of Timoshenko beams. A FEM approach was used by Benjeddou *et.al.* [12] to model a sandwich beam with shear and extension piezoelectric elements. The finite element model employed the displacement field of Zhang and Sun [51]. It was shown that the finite element results agree quite well with the analytical results. Deflection analysis of beams with extension and shear PZT patches using discontinuity functions was proposed by Ahmed and Osama in [5]. Raja *et.al.* [34] extended the finite element model of Benjeddou's research team to include a vibration control scheme. An improved 2-node Timoshenko beam model was presented by Kosmatka and Friedman [28]. Azulay and Abramovich [6] have presented analytical formulation and closed form solutions of composite beams with piezoelectric actuators. Abramovich and Lishvits [1] did extensive work on cross-ply beams to control the free vibrations. The work done by Kosmatka and Friedman [28], Azulay and Abramovich [6], Abramovich and Lishvits [1] is used in this paper for developing the control technique for the vibration suppression of the flexible structures.

The outline of the paper is as follows. A brief review of related literature about the mathematical models of beams and their control strategies was given in the introductory section. Section 2 gives an overview into the mathematical modeling

(sensor / actuator model, finite element model, state space model) of the smart cantilever beam. Controller design for the developed 4 SISO state space models of the smart plant in Section 2 is given in Section 3 with a deep insight into the design of the multirate output feedback based discrete sliding mode control algorithm using Bartoszewicz law. The simulation results are presented in Section 4. Conclusions are drawn in Section 5 followed by the references.

## II. MATHEMATICAL MODELING OF THE SMART BEAM

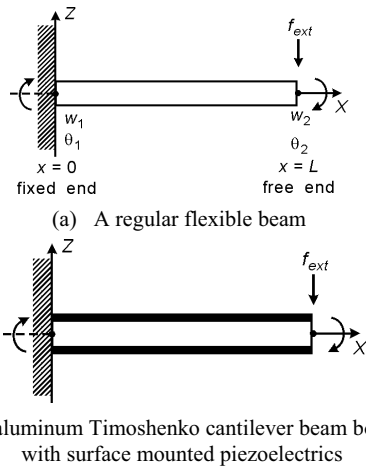


Fig. 1 A regular flexible beam and a smart aluminum Timoshenko cantilever beam bonded with surface mounted piezoelectrics

Few researchers have well established a mathematical finite element E-B model. These models do not consider the shear effects, axial effects, etc.,... Modeling of smart structures by shear deformable (Timoshenko) theory is limited. In our work, the effect of shear has been considered in modeling. Consider a aluminum cantilever beam as shown in Fig. 1(a) divided into 4 finite elements as shown in Fig. 2. The piezoelectric element is bonded on one discrete section (one finite element) of the surface of the beam as surface mounted sensor / actuator pair. The piezoelectric beam element is obtained by sandwiching the regular beam element between two thin piezoelectric layers at discrete sections. The bottom layer is acting as a sensor and the top layer is acting as an actuator as shown in the Fig. 2.

The element is assumed to have two structural DOF's  $(w, \theta)$  at each nodal point and an electrical DOF : a transverse deflection and an angle of rotation or slope. Since the voltage is constant over the electrode, the number of DOF is one for each element. The electrical DOF is used as a sensor voltage or actuator voltage. Corresponding to the two DOF's, a bending moment acts at each nodal point, i.e., counteracting moments are induced by the piezoelectric patches. The bending moment resulting from the voltage applied to the actuator adds a positive finite element bending moment, which is the moment at node 1, while subtracting it at node 2. In the *mathematical modeling* of the smart beam, the following assumptions are made. The mass and stiffness of

the adhesive used to bond the sensor / actuator pair to the master structure is being neglected. The smart cantilever beam model is developed using 1 piezoelectric beam element, which includes sensor and actuator dynamics and remaining beam elements as regular beam elements based on Timoshenko beam theory assumptions. The cable capacitance between the piezo patches and the signal-conditioning device is considered negligible and the temperature effects are neglected. The signal conditioning device gain is assumed as 100.

An external force input  $\mathbf{f}_{ext}$  (impulse) is applied at the free end of the smart beam. The beam is subjected to vibrations and takes a lot of time for the vibrations to dampen out. These vibrations are suppressed quickly in no time by the closed loop action of the controller, sensor and actuator. Thus, there are two inputs to the plant. One is the external force input  $\mathbf{f}_{ext}$  (impulse disturbance), which is taken as a load matrix of 1 unit in the simulation and the other input is the control input  $u$  to the actuator from the DSM controller. The dimensions and properties of the aluminum cantilever beam and piezoelectric sensor / actuator used are given in Tables I and II respectively.

TABLE I  
PROPERTIES OF THE FLEXIBLE CANTILEVER BEAM ELEMENT

Parameter (with units)	Symbol	Numerical values
Length (m)	$l_b$	0.5
Width (m)	$b$	0.024
Thickness (mm)	$t_b$	1
Young's modulus (GPa)	$E_b$	193.06
Density ( $\text{kg/m}^3$ )	$\rho_b$	8030
Damping constants	$\alpha, \beta$	0.001, 0.0001

TABLE II  
PROPERTIES OF THE PIEZO - SENSOR / ACTUATOR ELEMENT

Parameter (with units)	Symbol	Numerical values
Length (m)	$l_p$	0.125
Width (m)	$b$	0.024
Thickness (mm)	$t_a, t_s$	0.5
Young's modulus (GPa)	$E_p$	68
Density ( $\text{kg/m}^3$ )	$\rho_p$	7700
Piezo strain constant (m/V)	$d_{31}$	$125 \times 10^{-12}$

### A. Finite Element Modeling of the Regular Beam Element

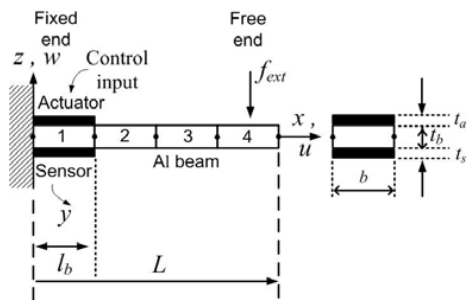
A regular beam element is shown in Fig. 1(a). The longitudinal axis of the regular beam element lies along the X-axis. The element has constant moment of inertia, modulus of elasticity, mass density and length [1], [6], [28], [30]. The displacement relations in the  $x, y$  and  $z$  directions of the beam can be written as

$$u(x, y, z, t) = z\theta(x, t) = z\left(\frac{\partial w}{\partial x} - \beta(x)\right), \quad (1)$$

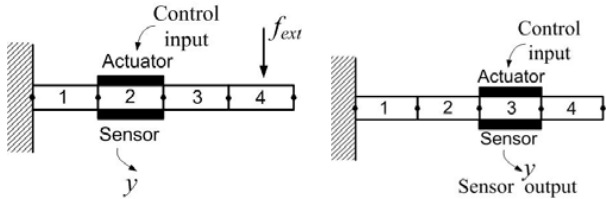
$$v(x, y, z, t) = 0, \quad (2)$$

$$w(x, y, z, t) = w(x, t), \quad (3)$$

where  $w$  is the time dependent transverse displacement of the centroidal axis (along  $z$  axis),  $\theta$  is the time dependent rotation of the cross-section about  $y$  axis,  $u$  is the axial displacement along the  $x$  axis,  $v$  is the lateral displacement along the  $y$  axis which is equal to zero. The total slope of the beam consists of two parts, one due to bending, which is  $(\partial w / \partial x)$  and the other due to shear, which is  $\beta(x)$ . The axial displacement of a point at a distance  $z$  from the centre line is only due to the bending slope and the shear slope has no contribution to this.

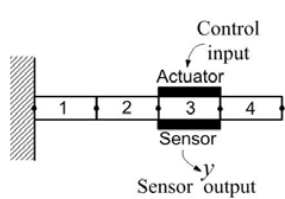


(a) Model 1 ( PZT placed at FE position 1, fixed end)



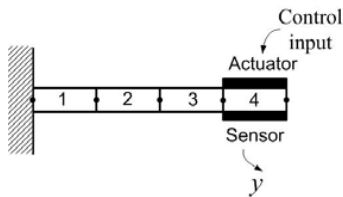
(b) Model 2

( PZT placed at FE position 2)



(c) Model 3

( PZT placed at FE position 3)



(d) Model 4 ( PZT placed at FE position 4, free end)

Fig. 2 A SISO smart Timoshenko beam divided into 4 finite elements and the sensor / actuator pair moved from fixed end to free end (Four SISO models of the same plant)

$\therefore$ , the strain components of the beam are given as

$$\varepsilon_{xx} = \frac{\partial u}{\partial x} = \frac{\partial u}{\partial \theta} \frac{\partial \theta}{\partial x} = z \frac{\partial \theta}{\partial x}, \quad (4)$$

$$\varepsilon_{yy} = \frac{\partial v}{\partial y} = 0, \quad (5)$$

$$\varepsilon_{zz} = \frac{\partial w}{\partial z} = 0, \quad (6)$$

where  $\varepsilon_{xx}, \varepsilon_{yy}, \varepsilon_{zz}$  are the longitudinal strains or the tensile strains in the 3 directions, i.e., in the  $x, y, z$  directions. The shear strains  $\gamma$  induced in the beam along the 3 directions (viz., along  $x, y, z$  directions) are given by

$$\gamma_{xz} = \frac{1}{2} \left[ \frac{\partial u}{\partial z} + \frac{\partial w}{\partial x} \right] = \frac{1}{2} \left[ \theta + \frac{\partial w}{\partial x} \right], \quad (7)$$

$$\gamma_{yz} = \frac{1}{2} \left[ \frac{\partial v}{\partial z} + \frac{\partial w}{\partial y} \right] = 0, \quad (8)$$

$$\gamma_{xy} = \frac{1}{2} \left[ \frac{\partial u}{\partial y} + \frac{\partial v}{\partial x} \right] = 0. \quad (9)$$

The effect of shear strains along  $y$  and  $z$  directions is equal to zero. Thus, the stresses in the beam element are given as

$$\sigma_{xx} = E_b \varepsilon_{xx} = E_b z \frac{\partial \theta}{\partial x}, \quad (10)$$

$$\sigma_{xz} = G \gamma_{xz} = \frac{1}{2} G \left[ \frac{\partial w}{\partial x} + \theta \right] = K \left[ \frac{\partial w}{\partial x} + \theta \right], \quad (11)$$

where  $E_b$  is the young's modulus of the beam material,  $G$  is shear modulus (or modulus of rigidity) of the beam material,  $\sigma_{xz}$  is the shear stress,  $\sigma_{xx}$  is the tensile stress and  $K$  is the shear coefficient [16] which depends on the material definition and on the cross sectional geometry, usually taken equal to  $5/6$ . The strain energy of the beam element depends upon the linear strain  $\varepsilon$ , the shear strain  $\gamma$  and is given by

$$U = \frac{1}{2} E_b I_b \left( \frac{\partial \theta}{\partial x} \right)^2 + \frac{1}{2} K G A_b \left( \frac{\partial w}{\partial x} + \theta \right)^2 \quad (12)$$

and the total strain energy is finally written as

$$U = \frac{1}{2} \int_0^{l_b} \begin{bmatrix} \frac{\partial \theta}{\partial x} \\ \frac{\partial w}{\partial x} + \theta \end{bmatrix}^T \begin{bmatrix} E_b I_b & 0 \\ 0 & K G A_b \end{bmatrix} \begin{bmatrix} \frac{\partial \theta}{\partial x} \\ \frac{\partial w}{\partial x} + \theta \end{bmatrix} dx, \quad (13)$$

where  $I_b$  is the mass moment of inertia of the beam element,  $A_b$  is the area of cross section of the beam element and  $l_b$  is the length of the beam. The kinetic energy  $T$  of the beam element depends on the sum of the kinetic energy due to the linear velocity  $\dot{w}$  and due to angular twist  $\dot{\theta}$  and is given by

$$T = \frac{1}{2} \rho_b A_b \left( \frac{\partial w}{\partial t} \right)^2 + \frac{1}{2} \rho_b I_b \left( \frac{\partial \theta}{\partial t} \right)^2 \quad (14)$$

and the total kinetic energy is finally written as

$$T = \frac{1}{2} \int_0^{l_b} \begin{bmatrix} \frac{\partial w}{\partial t} \\ \frac{\partial \theta}{\partial t} \end{bmatrix}^T \begin{bmatrix} \rho_b A_b & 0 \\ 0 & \rho_b I_b \end{bmatrix} \begin{bmatrix} \frac{\partial w}{\partial t} \\ \frac{\partial \theta}{\partial t} \end{bmatrix} dx, \quad (15)$$

where  $\rho_b$  is the mass density of the beam material. The total work done due to the external forces in the system is given by

$$W_e = \int_0^L \begin{bmatrix} w \\ \theta \end{bmatrix}^T \begin{bmatrix} q_d \\ m \end{bmatrix} dx, \quad (16)$$

where  $q_d$  represents distributed force along the length of the beam and  $m$  represents the moment along the length of the beam.

The equation of motion is derived using the concept of the total strain energy being equal to the sum of the change in the kinetic energy and the work done due to the external forces and is given by the Hamilton's principle as

$$\delta \Pi = \int_{t_1}^{t_2} (\delta U - \delta T - \delta W_e) dt = 0. \quad (17)$$

Here,  $\delta U$ ,  $\delta T$  and  $\delta W_e$  are the variations of the strain energy, the kinetic energy, work done due to the external forces and  $T$  is kinetic energy,  $U$  is strain energy,  $W$  is the external work done and  $t$  is the time.

Substituting the values of strain energy from Eq. (13), kinetic energy from Eq. (15) and external work done from Eq. (16) in Eq. (17) and integrating by parts, we get the governing equation of motion (Timoshenko beam equations) of a general shaped beam modeled with Timoshenko beam theory as

$$\frac{\partial \left\{ K G A_b \left( \frac{\partial w}{\partial x} + \theta \right) \right\}}{\partial x} + q_d = \rho_b A_b \frac{\partial^2 w}{\partial t^2}, \quad (18)$$

$$\frac{\partial \left\{ E_b I_b \frac{\partial \theta}{\partial x} \right\}}{\partial x} - K G A_b \left( \frac{\partial w}{\partial x} + \theta \right) + m = \rho_b I_b \frac{\partial^2 \theta}{\partial t^2}. \quad (19)$$

The R.H.S. of Eq. (18) is the time derivative of the linear momentum, whereas the R.H.S. of Eq. (19) is the time derivative of the moment of momentum.

For the static case with no external force acting on the beam, the governing equation of motion (Timoshenko beam equations) reduces to

$$\frac{\partial \left\{ K G A_b \left( \frac{\partial w}{\partial x} + \theta \right) \right\}}{\partial x} = 0 \quad (20)$$

and

$$\frac{\partial \left\{ E_b I_b \frac{\partial \theta}{\partial x} \right\}}{\partial x} - K G A_b \left( \frac{\partial w}{\partial x} + \theta \right) = 0. \quad (21)$$

From Eq. (21), it can be seen that this governing equation of the beam based on Timoshenko beam theory can only be satisfied if the polynomial order for  $w$  is selected one order higher than the polynomial order for  $\theta$ . Let  $w$  be approximated by a cubic polynomial and  $\theta$  be approximated by a quadratic polynomial as

$$w = a_1 + a_2 x + a_3 x^2 + a_4 x^3, \quad (22)$$

$$\theta = b_1 + b_2 x + b_3 x^2. \quad (23)$$

Here, in (22) and (23),  $x$  is the distance of the finite element node from the fixed end of the beam,  $a_i$  and  $b_j$  ( $i=1,2,3,4$ ) and ( $j=1,2,3$ ) are the unknown coefficients and are found out using the boundary conditions at the beam element ends  $x = (0, l_b)$  as

$$\text{at } x=0, \quad w=w_1, \quad \theta=0 \quad (24)$$

$$\text{and at } x=l_b, \quad w=w_2, \quad \theta=-\theta_2. \quad (25)$$

After applying boundary conditions from Eqs. (24), (25) on (22), (23), the unknown coefficients  $a_i$  and  $b_j$  can be solved.

Substituting the obtained unknown coefficients  $a_i$  and  $b_j$  in Eqs. (22), (23) and writing them in matrix form, we get, the transverse displacement, the first spatial derivative of the transverse displacement, the second spatial derivative of the transverse displacement and the time derivative of Eq. (22) as

$$[w(x,t)] = [N_w][\mathbf{q}], \quad (26)$$

$$[w'(x,t)] = [N_\theta][\mathbf{q}], \quad (27)$$

$$[w''(x,t)] = [N_a][\mathbf{q}], \quad (28)$$

$$[\dot{w}(x,t)] = [N_w][\dot{\mathbf{q}}], \quad (29)$$

where  $\mathbf{q}$  is the vector of displacements and slopes,  $\dot{\mathbf{q}}$  is the time derivative of the modal coordinate vector,  $[N_w]^T$ ,  $[N_\theta]^T$ ,  $[N_a]^T$  are the shape functions (for displacement, rotations and accelerations) taking the shear  $\phi$  into consideration and are given as

$$[N_w]^T = \begin{bmatrix} \frac{1}{(1+\phi)} \left\{ 2 \left( \frac{x}{l_b} \right)^3 - 3 \left( \frac{x}{l_b} \right)^2 - \phi \left( \frac{x}{l_b} \right) + (1+\phi) \right\} \\ \frac{L}{(1+\phi)} \left\{ \left( \frac{x}{l_b} \right)^3 - \left( 2 + \frac{\phi}{2} \right) \left( \frac{x}{l_b} \right)^2 + \left( 1 + \frac{\phi}{2} \right) \left( \frac{x}{l_b} \right) \right\} \\ - \frac{1}{(1+\phi)} \left\{ 2 \left( \frac{x}{l_b} \right)^3 - 3 \left( \frac{x}{l_b} \right)^2 - \phi \left( \frac{x}{l_b} \right) \right\} \\ \frac{l_b}{(1+\phi)} \left\{ \left( \frac{x}{l_b} \right)^3 - \left( 1 - \frac{\phi}{2} \right) \left( \frac{x}{l_b} \right)^2 - \left( \frac{\phi}{2} \right) \left( \frac{x}{l_b} \right) \right\} \end{bmatrix}, \quad (30)$$

$$[N_\theta]^T = \begin{bmatrix} \frac{6}{(1+\phi)l_b} \left\{ \left( \frac{x}{l_b} \right)^2 - \left( \frac{x}{l_b} \right) - \frac{\phi(1+\phi)}{6} + \frac{(1+\phi)^2 l_b}{6} \right\} \\ \frac{1}{(1+\phi)} \left\{ 3 \left( \frac{x}{l_b} \right)^2 - (4+\phi) \left( \frac{x}{l_b} \right) + (1+\phi) \right\} \\ - \frac{6}{(1+\phi)l_b} \left\{ \left( \frac{x}{l_b} \right)^2 - \left( \frac{x}{l_b} \right) \right\} \\ \frac{1}{(1+\phi)} \left\{ 3 \left( \frac{x}{l_b} \right)^2 - (2-\phi) \left( \frac{x}{l_b} \right) \right\} \end{bmatrix}, \quad (31)$$

$$[N_a]^T = \begin{bmatrix} \frac{6}{(1+\phi)l_b} \left\{ \frac{2x}{l_b^2} - \frac{1}{l_b} \right\} \\ \frac{1}{(1+\phi)l_b} \left\{ \frac{6x}{l_b} - (4+\phi) \right\} \\ -\frac{6}{(1+\phi)l_b} \left\{ \frac{6x}{l_b^2} - \frac{1}{l_b} \right\} \\ \frac{1}{(1+\phi)} \left\{ \frac{6x}{l_b^2} - \left( \frac{2-\phi}{l_b} \right) \right\} \end{bmatrix}, \quad (32)$$

where  $[N_\theta] = [N_w]'$ ,  $[N_a] = [N_w]''$  and  $\phi$  is the ratio of the beam bending stiffness to shear stiffness and is given by

$$\phi = \frac{12}{l_b^2} \left( \frac{E_b I_b}{K G A_b} \right). \quad (33)$$

The mass matrix of the regular beam element (also called as the local mass matrix) is the sum of the translational mass and the rotational mass and is given in matrix form as

$$[M^b] = \int_0^{l_b} \begin{bmatrix} [N_w] \\ [N_\theta] \end{bmatrix}^T \begin{bmatrix} \rho_b A_b & 0 \\ 0 & \rho_b I_{yy} \end{bmatrix} \begin{bmatrix} [N_w] \\ [N_\theta] \end{bmatrix} dx. \quad (34)$$

Substituting the mode shape functions  $[N_w]$ ,  $[N_\theta]$  into (34) and integrating, we get the mass matrix of the regular beam element as

$$[M^b] = [M_{\rho_b A_b}] + [M_{\rho_b I_b}], \quad (35)$$

where  $[M_{\rho_b A_b}]$  and  $[M_{\rho_b I_b}]$  in Eq. (35) is associated with the translational inertia and rotary inertia (with shear) as

$$[M_{\rho_b A_b}] = \frac{\rho_b I_b}{210(1+\phi)^2} \begin{bmatrix} (70\phi^2 + 147\phi + 78) & (35\phi^2 + 77\phi + 44)\frac{l_b}{4} \\ (35\phi^2 + 77\phi + 44)\frac{l_b}{4} & (7\phi^2 + 14\phi + 8)\frac{l_b^2}{4} \\ (35\phi^2 + 63\phi + 27) & (35\phi^2 + 63\phi + 26)\frac{l_b}{4} \\ -(35\phi^2 + 63\phi + 26)\frac{l_b}{4} & -(7\phi^2 + 14\phi + 6)\frac{l_b^2}{4} \\ (35\phi^2 + 63\phi + 27) & -(35\phi^2 + 63\phi + 26)\frac{l_b}{4} \\ (35\phi^2 + 63\phi + 26)\frac{l_b}{4} & -(7\phi^2 + 14\phi + 6)\frac{l_b^2}{4} \\ (70\phi^2 + 147\phi + 78) & -(35\phi^2 + 77\phi + 44)\frac{l_b}{4} \\ -(35\phi^2 + 77\phi + 44)\frac{l_b}{4} & (7\phi^2 + 14\phi + 8)\frac{l_b^2}{4} \end{bmatrix}, \quad (36)$$

$$[M_{\rho_b I_b}] = \frac{\rho_b I_b}{30(1+\phi)^2 l_b} \begin{bmatrix} 36 & -(15\phi - 3)l_b \\ -(15\phi - 3)l_b & (10\phi^2 + 5\phi + 4)l_b^2 \\ (10\phi^2 + 5\phi + 4)l_b^2 & (15\phi - 3)l_b \\ -(15\phi - 3)l_b & (5\phi^2 - 5\phi - 1)l_b^2 \\ -36 & -(15\phi - 3)l_b \\ (15\phi - 3)l_b & (5\phi^2 - 5\phi - 1)l_b^2 \\ 36 & (15\phi - 3)l_b \\ (15\phi - 3)l_b & (10\phi^2 + 5\phi + 4)l_b^2 \end{bmatrix}. \quad (37)$$

The stiffness matrix  $[K^b]$  of the regular beam element (local stiffness matrix) is the sum of the bending stiffness and the shear stiffness and is written in matrix form as

$$[K^b] = \int_0^{l_b} \begin{bmatrix} \frac{\partial}{\partial x}[N_\theta] \\ [N_\theta] + \frac{\partial}{\partial x}[N_w] \end{bmatrix}^T \begin{bmatrix} E_b I_b & 0 \\ 0 & K G A_b \end{bmatrix} \begin{bmatrix} \frac{\partial}{\partial x}[N_\theta] \\ [N_\theta] + \frac{\partial}{\partial x}[N_w] \end{bmatrix} dx. \quad (38)$$

Substituting the mode shape functions  $[N_w]$ ,  $[N_\theta]$  into (38) and integrating, we get the stiffness matrix of the regular beam element as  $[K^b]$  which is given by

$$[K^b] = \frac{E_b I_b}{(1+\phi)l_b^3} \begin{bmatrix} 12 & 6l_b & -12 & 6l_b \\ 6l_b & (4+\phi)l_b^2 & -6l_b & (2-\phi)l_b^2 \\ -12 & -6l_b & 12 & -6l_b \\ 6l_b & (2-\phi)l_b^2 & -6l_b & (4+\phi)l_b^2 \end{bmatrix} \quad (39)$$

### B. Finite Element Modeling of Piezoelectric Beam Element

The finite element modeling of the piezoelectric element is done as follows. The regular beam and the piezoelectric beam (beam + piezo-patch) are shown in Figs. 1(a) and 1(b) respectively. The piezoelectric beam element is obtained by bonding the regular beam element with a layer of two piezoelectric patches or layers, one above and the other below at two finite element positions as a collocated pair as shown in the Figs. 2(a) - (d). Collocated piezoelectric sensor / actuators are used because they are supposed to be more robust (against parameter uncertainty) under feedback control action.

The bottom layer acts as the sensor and the top layer acts as an actuator. The element is assumed to have two structural degrees of freedom (DOF) at each nodal point, which are, transverse deflection  $w$ , an angle of rotation or slope  $\theta$  and an electrical degree of freedom, i.e., the sensor voltage. The piezo sensor-actuator pair is also modeled using the Timoshenko beam theory. Employing the same procedure similar to the regular beam element, which was modeled using the Timoshenko beam theory, we obtain the mass matrix of the piezoelectric element as

$$M^p = [M_{\rho_p A_p}] + [M_{\rho_p I_p}], \quad (40)$$

where

$\rho_p$  is the mass density of piezoelectric element,

$A_p$  is the area of the piezoelectric patch =  $2t_a b$ , i.e., the area of the sensor as well as actuator,

$b$  being the width of the beam / width of the sensor / actuator,

$l_p$  is the length of the piezoelectric patch.

Here, in Eqn. (40),  $[M_{\rho_p A_p}]$  and  $[M_{\rho_p I_p}]$  is associated with the translational inertia and the rotary inertia of the piezoelectric element as

$$[M_{\rho_p A_p}] = \frac{\rho_p A_p I_p}{210(1+\phi)^2} \begin{bmatrix} (70\phi^2 + 147\phi + 78) \frac{I_p}{4} & (35\phi^2 + 77\phi + 44) \frac{I_p^2}{4} \\ (35\phi^2 + 77\phi + 44) \frac{I_p}{4} & (7\phi^2 + 14\phi + 8) \frac{I_p^2}{4} \\ (35\phi^2 + 63\phi + 27) & (35\phi^2 + 63\phi + 26) \frac{I_p}{4} \\ -(35\phi^2 + 63\phi + 26) \frac{I_p}{4} & -(7\phi^2 + 14\phi + 6) \frac{I_p^2}{4} \\ (35\phi^2 + 63\phi + 27) & -(35\phi^2 + 63\phi + 26) \frac{I_p}{4} \\ (35\phi^2 + 63\phi + 27) \frac{I_p}{4} & -(7\phi^2 + 14\phi + 6) \frac{I_p^2}{4} \\ (70\phi^2 + 147\phi + 78) & -(35\phi^2 + 77\phi + 44) \frac{I_p}{4} \\ -(35\phi^2 + 77\phi + 44) \frac{I_p}{4} & (7\phi^2 + 14\phi + 8) \frac{I_p^2}{4} \end{bmatrix} \quad (41)$$

and

$$[M_{\rho_p I_p}] = \frac{\rho_p I_p}{30(1+\phi)^2 l_p} \begin{bmatrix} 36 & -(15\phi-3) l_p \\ -(15\phi-3) l_p & (10\phi^2+5\phi+4) l_p^2 \\ (10\phi^2+5\phi+4) l_p^2 & (15\phi-3) l_p \\ -(15\phi-3) l_p & (5\phi^2-5\phi-1) l_p^2 \\ -36 & -(15\phi-3) l_p \\ (15\phi-3) l_p & (5\phi^2-5\phi-1) l_p^2 \\ 36 & (15\phi-3) l_p \\ (15\phi-3) l_p & (10\phi^2+5\phi+4) l_p^2 \end{bmatrix} \quad (42)$$

Similarly, we obtain the stiffness matrix  $[K^{piezo}]$  of the piezoelectric element as

$$[K^p] = \frac{E_p I_p}{(1+\phi) l_p^3} \begin{bmatrix} 12 & 6 l_p & -12 & 6 l_p \\ 6 l_p & (4+\phi) l_p^2 & -6 l_p & (2-\phi) l_p^2 \\ -12 & -6 l_p & 12 & -6 l_p \\ 6 l_p & (2-\phi) l_p^2 & -6 l_p & (4+\phi) l_p^2 \end{bmatrix} \quad (43)$$

where

$$EI = E_b I_b + 2 E_p I_p, \quad (44)$$

$$\rho A = b(\rho_b t_b + 2 \rho_p t_a), \quad (45)$$

$$I_p = \frac{1}{12} b t_a^3 + b t_a \left( \frac{t_a + t_b}{2} \right)^2. \quad (46)$$

Here,  $E_p$  is the modulus of elasticity of the piezoelectric material,  $A_p$  is the area of the piezoelectric patch  $\rho_p$  is the mass density of the piezoelectric material,  $I_p$  is the moment of inertia of the piezoelectric layer with respect to the neutral axis of the beam,  $t_p$  is the thickness of the beam and  $t_a$  is the thickness of the actuator, which is also equal to the thickness of the sensor  $t_s$  and  $b$  is the width of the piezo-patch and also that of the host beam.

### C. Mass and Stiffness of Beam Element with Piezo Patch

The mass and stiffness matrix for the piezoelectric beam element (regular beam element with piezoelectric patches placed at the top and bottom surfaces) as a collocated pair (element 1 in Fig. 2(a)) is given by

$$[M] = [M^b] + [M^p] \quad (47)$$

$$[K] = [K^b] + [K^p]. \quad (48)$$

Assembly of the regular beam element and the piezoelectric element is done by adding the two matrices. It is assumed that the rotations and displacements are the same in all the layers of the structure.

### D. Piezoelectric Sensors and Actuators

The linear piezoelectric coupling between the elastic field and the electric field of a PZT material is expressed by the direct and converse piezoelectric constitutive equations as

$$D = d \sigma + e^T E_f, \quad (49)$$

$$\varepsilon = s^E \sigma + d E_f, \quad (50)$$

where  $\sigma$  is the stress,  $\varepsilon$  is the strain,  $E_f$  is the electric field,  $D$  is the dielectric displacement,  $e$  is the permittivity of the medium,  $s^E$  is the compliance of the medium, and  $d$  is the piezoelectric constant [35].

#### 1) Sensor Equation

The direct piezoelectric equation is used to calculate the output charge produced by the strain in the structure. The total charge  $Q(t)$  developed on the sensor surface (due to the strain) is the spatial summation of all point charges developed on the sensor layer and the corresponding current generated is given by

$$i(t) = z e_{31} c \int_0^{l_p} N_a^T \dot{\mathbf{q}} dx, \quad (51)$$

where  $z = \frac{t_b}{2} + t_a$ ,  $e_{31}$  is the piezoelectric stress / charge constant,  $\dot{\mathbf{q}}$  is the time derivative of the modal coordinate vector and  $N_a^T$  is the second spatial derivative of the mode shape function of the beam. This current is converted into the open circuit sensor voltage  $V^s$  using a signal-conditioning device with gain  $G_c$  and applied to an actuator with the controller gain  $K_c$ . The sensor output voltage obtained is as

$$V^s = G_c e_{31} z c \int_0^{l_p} N_a^T \dot{\mathbf{q}} dx \quad (52)$$

or can be expressed as

$$V^s(t) = \mathbf{p}^T \dot{\mathbf{q}}, \quad (53)$$

where  $\mathbf{p}^T$  is a constant vector. The input voltage to the actuator is  $V^a(t)$  and is given by

$$V^a(t) = K_c G_c e_{31} z c \int_0^{l_p} N_a^T \dot{\mathbf{q}} dx. \quad (54)$$

Note that the sensor output is a function of the second spatial derivative of the mode shape.

## 2) Actuator equation

The actuator strain is derived from the converse piezoelectric equation. The strain developed by the applied electric field  $E_f$  on the actuator layer is given by

$$\varepsilon_A = d_{31} E_f = d_{31} \frac{V^a(t)}{t_a}. \quad (55)$$

When the input to the actuator  $V^a(t)$  is applied in the thickness direction, the stress developed is

$$\sigma_A = E_p d_{31} \frac{V^a(t)}{t_a}. \quad (56)$$

The resultant moment  $M_A$  acting on the beam due to the stress is determined by integrating the stress through the structure thickness as

$$M_A = E_p d_{31} \bar{z} V^a(t), \quad (57)$$

where  $\bar{z}$ , is the distance between the neutral axis of the beam and the piezoelectric layer. The bending moment results in the generation of the control force. Finally, the control force applied by the actuator is obtained as

$$\mathbf{f}_{ctrl} = E_p d_{31} c \bar{z} \int_0^{l_p} N_\theta dx V^a(t) \quad (58)$$

or can be expressed as

$$\mathbf{f}_{ctrl} = \mathbf{h} V^a(t), \quad (59)$$

where  $[N_\theta]^T$  is the first spatial derivative of mode shape function of the beam and  $\mathbf{h}^T$  is a constant vector which depends on the piezo characteristics and its location on the beam. If an external force  $\mathbf{f}_{ext}$  (impulse disturbance) acts on the beam, then, the total force vector becomes

$$\mathbf{f}^t = \mathbf{f}_{ext} + \mathbf{f}_{ctrl}. \quad (60)$$

## E. Dynamic Equation of the Smart Structure

The dynamic equation of the smart structure is obtained by using both the regular and piezoelectric beam elements (local matrices) given by (35), (39), (40), (41)-(43) and (47), (48). The mass and stiffness of the bonding or the adhesive between the master structure and the sensor / actuator pair is neglected. The mass and stiffness of the entire beam, which is divided into 4 finite elements with the piezo-patches placed at only one discrete location at a time is assembled using the FEM technique [39] and the assembled matrices (global matrices),  $\mathbf{M}$  and  $\mathbf{K}$  are obtained. The equation of motion of the smart structure is finally given by

$$\mathbf{M} \ddot{\mathbf{q}} + \mathbf{K} \mathbf{q} = \mathbf{f}_{ext} + \mathbf{f}_{ctrl} = \mathbf{f}^t, \quad (61)$$

where  $\mathbf{M}$ ,  $\mathbf{K}$ ,  $\mathbf{f}_{ext}$ ,  $\mathbf{f}_{ctrl}$ ,  $\mathbf{f}^t$  are the global mass matrix, global stiffness matrix of the smart beam, the external force applied to the beam, the controlling force from the actuator and the total force coefficient vector respectively. The generalized coordinates are introduced into Eq. (61) using a transformation  $\mathbf{q} = \mathbf{T} \mathbf{g}$  in order to reduce it further such that the resultant equation represents the dynamics of the first 2 vibratory modes of the smart flexible cantilever beam.  $\mathbf{T}$  is the modal matrix containing the eigen vectors representing the first 2 vibratory modes. This method is used to derive the uncoupled equations governing the motion of the free vibrations of the system in terms of principal coordinates by introducing a linear transformation between the generalized coordinates  $\mathbf{q}$  and the principal coordinates  $\mathbf{g}$ . Equation (61) now becomes

$$\mathbf{M} \mathbf{T} \ddot{\mathbf{g}} + \mathbf{K} \mathbf{T} \mathbf{g} = \mathbf{f}_{ext} + \mathbf{f}_{ctrl}. \quad (62)$$

Multiplying Eq. (62) by  $\mathbf{T}^T$  on both sides and further simplifying, we get

$$\mathbf{M}^* \ddot{\mathbf{g}} + \mathbf{K}^* \mathbf{g} = \mathbf{f}_{ext}^* + \mathbf{f}_{ctrl}^*, \quad (63)$$

where  $\mathbf{M}^* = \mathbf{T}^T \mathbf{M} \mathbf{T}$ ,  $\mathbf{K}^* = \mathbf{T}^T \mathbf{K} \mathbf{T}$ ,  $\mathbf{f}_{ext}^* = \mathbf{T}^T \mathbf{f}_{ext}$  and  $\mathbf{f}_{ctrl}^* = \mathbf{T}^T \mathbf{f}_{ctrl}$ .

Here, the various parameters like  $\mathbf{M}^*$ ,  $\mathbf{K}^*$ ,  $\mathbf{f}_{ext}^*$ ,  $\mathbf{f}_{ctrl}^*$  in Eq. (63) represents the generalized mass matrix, the generalized stiffness matrix, the generalized external force vector and the generalized control force vector respectively. The generalized structural modal damping matrix  $\mathbf{C}^*$  is introduced into Eq. (63) by using

$$\mathbf{C}^* = \alpha \mathbf{M}^* + \beta \mathbf{K}^*, \quad (64)$$

where  $\alpha$  and  $\beta$  are the frictional damping constant and the structural damping constant used in  $\mathbf{C}^*$ . The dynamic equation of the smart flexible cantilever beam developed is obtained as

$$\mathbf{M}^* \ddot{\mathbf{g}} + \mathbf{C}^* \dot{\mathbf{g}} + \mathbf{K}^* \mathbf{g} = \mathbf{f}_{ext}^* + \mathbf{f}_{ctrl}^*. \quad (65)$$

## F. State Space Model of the Smart Structure

The state space model of the smart flexible cantilever beam is obtained as follows [30], [63].

$$\text{Let } \mathbf{g} = \begin{bmatrix} x_1 \\ x_2 \end{bmatrix} \Rightarrow \dot{\mathbf{g}} = \begin{bmatrix} \dot{x}_1 \\ \dot{x}_2 \end{bmatrix} = \begin{bmatrix} x_3 \\ x_4 \end{bmatrix}, \quad (66)$$

$$\text{Thus, } \dot{x}_1 = x_3, \quad \dot{x}_2 = x_4 \quad (67)$$

and Eq. (65) now becomes

$$\mathbf{M}^* \begin{bmatrix} \dot{x}_3 \\ \dot{x}_4 \end{bmatrix} + \mathbf{C}^* \begin{bmatrix} x_3 \\ x_4 \end{bmatrix} + \mathbf{K}^* \begin{bmatrix} x_1 \\ x_2 \end{bmatrix} = \mathbf{f}_{ext}^* + \mathbf{f}_{ctrl}^*, \quad (68)$$



which can be further simplified as

$$\begin{bmatrix} \dot{x}_3 \\ \dot{x}_4 \end{bmatrix} = -\mathbf{M}^{*-1} \mathbf{K}^* \begin{bmatrix} x_1 \\ x_2 \end{bmatrix} - \mathbf{M}^{*-1} \mathbf{C}^* \begin{bmatrix} x_3 \\ x_4 \end{bmatrix} + \mathbf{M}^{*-1} \mathbf{f}_{ext}^* + \mathbf{M}^{*-1} \mathbf{f}_{ctrl}^* \quad (69)$$

The generalized external force coefficient vector is

$$\mathbf{f}_{ext}^* = \mathbf{T}^T \mathbf{f}_{ext} = \mathbf{T}^T \mathbf{f} r(t), \quad (70)$$

where  $r(t)$  is external force input (impulse disturbance) to the beam. The generalized control force coefficient vector is

$$\mathbf{f}_{ctrl}^* = \mathbf{T}^T \mathbf{f}_{ctrl} = \mathbf{T}^T \mathbf{h} V^a(t) = \mathbf{T}^T \mathbf{h} u(t) \quad (71)$$

where the voltage  $V^a(t)$  is the input voltage to the actuator from the controller and is nothing but the control input  $u(t)$  to the actuator,  $\mathbf{h}$  is a constant vector which depends on the actuator type, its characteristics and its position on the beam and is given by

$$\begin{aligned} \mathbf{h}_2 &= E_p d_{31} b \bar{z} [-1 \ 1 \ \dots \dots \ 0 \ 0]_{8 \times 1}, \\ &= a_c [-1 \ 1 \ \dots \dots \ 0 \ 0] \end{aligned} \quad (72)$$

for one piezoelectric actuator element (say, for the piezo patch placed at the finite element position numbering 2), where  $E_p d_{31} b \bar{z} = a_c$  being the actuator constant.

So, using Eqs. (67), (70) and (71) in Eq. (69), the state space equation for the smart beam for 2 vibratory modes is represented as

$$\begin{bmatrix} \dot{x}_1 \\ \dot{x}_2 \\ \dot{x}_3 \\ \dot{x}_4 \end{bmatrix} = \begin{bmatrix} 0 & I \\ -\mathbf{M}^{*-1} \mathbf{K}^* & -\mathbf{M}^{*-1} \mathbf{C}^* \end{bmatrix} \begin{bmatrix} x_1 \\ x_2 \\ x_3 \\ x_4 \end{bmatrix} + \begin{bmatrix} 0 \\ \mathbf{M}^{*-1} \mathbf{T}^T \mathbf{h} \end{bmatrix} \mathbf{u}(t) + \begin{bmatrix} 0 \\ \mathbf{M}^{*-1} \mathbf{T}^T \mathbf{f} \end{bmatrix} r(t) \quad (73)$$

$$\text{i.e.,} \quad \dot{\mathbf{X}} = \mathbf{A} \mathbf{x}(t) + \mathbf{B} \mathbf{u}(t) + \mathbf{E} r(t). \quad (74)$$

The sensor voltage is taken as the output of the system and its equation (output equation) is obtained as

$$V^s(t) = \mathbf{p}^T \dot{\mathbf{q}} = y(t), \quad (75)$$

where  $\mathbf{p}^T$  is a constant vector which depends on the piezoelectric sensor characteristics and on the location of the piezo sensor on the beam and is given by

$$\begin{aligned} \mathbf{p}_4^T &= G_c e_{31} z b [0 \ 0 \ \dots \dots \ -1 \ 1]_{1 \times 8}, \\ &= S_c [0 \ 0 \ \dots \dots \ -1 \ 1], \end{aligned} \quad (76)$$

for the piezo-patch placed at finite element location 4 and  $G_c e_{31} z b = S_c$  is the sensor constant. Thus, the sensor output equation for a SISO case is given by

$$y(t) = \mathbf{p}^T \dot{\mathbf{q}} = \mathbf{p}^T \mathbf{T} \dot{\mathbf{g}} = \mathbf{p}^T \mathbf{T} \begin{bmatrix} \dot{x}_3 \\ \dot{x}_4 \end{bmatrix}, \quad (77)$$

which can be finally written as

$$y(t) = \begin{bmatrix} 0 & \mathbf{p}^T \mathbf{T} \end{bmatrix} \begin{bmatrix} x_1 \\ x_2 \\ x_3 \\ x_4 \end{bmatrix}. \quad (78)$$

$$\text{i.e.,} \quad y(t) = \mathbf{C}^T \mathbf{x}(t) + \mathbf{D} u(t). \quad (79)$$

which is the output equation. The single input single output state space model (state equation and the output equation) of the smart structure developed for the system in (74) and (79) thus, is given by

$$\dot{\mathbf{x}} = \mathbf{A} \mathbf{x}(t) + \mathbf{B} u(t) + \mathbf{E} r(t), \quad y(t) = \mathbf{C}^T \mathbf{x}(t) + \mathbf{D} u(t), \quad (80)$$

with

$$\begin{aligned} \mathbf{A} &= \begin{bmatrix} 0 & I \\ -\mathbf{M}^{*-1} \mathbf{K}^* & -\mathbf{M}^{*-1} \mathbf{C}^* \end{bmatrix}_{(4 \times 4)}, \quad \mathbf{E} = \begin{bmatrix} 0 \\ \mathbf{M}^{*-1} \mathbf{T}^T \mathbf{f} \end{bmatrix}_{(4 \times 1)} \\ \mathbf{B} &= \begin{bmatrix} 0 \\ \mathbf{M}^{*-1} \mathbf{T}^T \mathbf{h} \end{bmatrix}_{(4 \times 1)}, \quad \mathbf{C}^T = \begin{bmatrix} 0 & \mathbf{p}^T \end{bmatrix}_{(1 \times 4)}, \\ \mathbf{D} &= \text{Null Matrix}, \end{aligned} \quad (81)$$

where the parameters  $r(t)$ ,  $\mathbf{u}(t)$ ,  $\mathbf{A}$ ,  $\mathbf{B}$ ,  $\mathbf{C}$ ,  $\mathbf{D}$ ,  $\mathbf{E}$ ,  $\mathbf{x}(t)$ ,  $y(t)$  represents the external force input, the control input, system matrix, input matrix, output matrix, transmission matrix, external load matrix, state vector and the system output (sensor output).

Since Timoshenko beam model is closer to the actual model, it is used as the basis for controller design in our research work. The state space model in Eq. (80) is obtained for various sensor / actuator locations on the cantilever beam by using 3 regular beam elements and 1 piezo electric element at a time as a collocated pair as shown in Fig. 2, thus giving rise to 4 SISO models of the smart beam system.

By placing a piezoelectric element as sensor / actuator at one finite element of the cantilever beam and making other elements as regular beam elements as shown in Fig. 2 and by varying the position of the piezoelectric sensor / actuator from the fixed end to the free end, various SISO state space models are obtained with the inclusion of mass and stiffness of the sensor / actuator. Then, the control of these models is obtained using the MROF based DSM control technique, which is considered, in the next section, thus, finally concluding the best model for vibration control.

State space model of the smart cantilever beam with sensor / actuator pair at element 1 (fixed end), i.e., the SISO model 1 is represented by Eqn. (80) with

$$A_1 = 1e4 * \begin{bmatrix} 0 & 0 & 0.0001 & 0 \\ 0 & 0 & 0 & 0.0001 \\ -5.5567 & 0.0000 & -0.0006 & 0.0000 \\ 0.0000 & -0.1637 & 0.0000 & -0.0000 \end{bmatrix},$$

$$B_1 = \begin{bmatrix} 0 \\ 0 \\ -0.0514 \\ -0.0027 \end{bmatrix}, \quad (82)$$

$$C_1^T = [0 \quad 0 \quad -0.0026 \quad -0.0010], \quad D_1 = 0,$$

$$E_1 = 1e3 * \begin{bmatrix} 0 \\ 0 \\ 3.0567 \\ -1.2241 \end{bmatrix}.$$

State space model of the smart cantilever beam with sensor / actuator pair at element 2 (fixed end), i.e., the SISO model 2 is represented by Eqn. (80) with

$$A_2 = 1e4 * \begin{bmatrix} 0 & 0 & 0.0001 & 0 \\ 0 & 0 & 0 & 0.0001 \\ -3.2159 & 0.0000 & -0.0003 & 0.0000 \\ 0.0000 & -0.1158 & 0.0000 & -0.0000 \end{bmatrix},$$

$$B_2 = \begin{bmatrix} 0 \\ 0 \\ -0.0862 \\ -0.0168 \end{bmatrix}, \quad (83)$$

$$C_2^T = 1e3 * [0 \quad 0 \quad 0.8572 \quad -0.5738], \quad D_2 = 0,$$

$$E_2 = 1e3 * \begin{bmatrix} 0 \\ 0 \\ 2.5605 \\ -0.9010 \end{bmatrix}.$$

State space model of the smart cantilever beam with sensor / actuator pair at element 3 (fixed end), i.e., the SISO model 3 is represented by Eqn. (80) with

$$A_3 = 1e4 * \begin{bmatrix} 0 & 0 & 0.0001 & 0 \\ 0 & 0 & 0 & 0.0001 \\ -3.8213 & -0.0000 & -0.0004 & -0.0000 \\ -0.0000 & -0.0839 & -0.0000 & -0.0000 \end{bmatrix},$$

$$B_3 = \begin{bmatrix} 0 \\ 0 \\ 0.0375 \\ -0.0198 \end{bmatrix}, \quad (84)$$

$$C_3^T = 1e3 * [0 \quad 0 \quad 0.0019 \quad -0.0003], \quad D_3 = 0,$$

$$E_3 = 1e3 * \begin{bmatrix} 0 \\ 0 \\ 2.6924 \\ -0.7842 \end{bmatrix}.$$

State space model of the smart cantilever beam with sensor / actuator pair at element 4 (fixed end), i.e., the SISO model 4 is represented by Eqn. (80) with

$$A_4 = 1e4 * \begin{bmatrix} 0 & 0 & 0.0001 & 0 \\ 0 & 0 & 0 & 0.0001 \\ -0.402 & 0.0000 & -0.0000 & -0.0000 \\ -0.0000 & -2.3620 & -0.0000 & -0.0002 \end{bmatrix},$$

$$B_4 = \begin{bmatrix} 0 \\ 0 \\ 0.0164 \\ -0.1822 \end{bmatrix}, \quad (85)$$

$$C_4^T = 1e-3 * [0 \quad 0 \quad 0.0208 \quad -0.2542], \quad D_4 = 0,$$

$$E_4 = 1e3 * \begin{bmatrix} 0 \\ 0 \\ 0.5449 \\ -1.4109 \end{bmatrix}.$$

The mode frequencies of the smart beam for all the 4 SISO models is shown in the Table III.

TABLE III  
CHARACTERISTICS OF THE 4 SISO MODELS

PZT location	First mode (Hz.)	Second mode (Hz.)
Model 1	6.7532	39.3458
Model 2	5.9325	31.2640
Model 3	4.9661	33.5070
Model 4	3.1094	23.8404

### III. REVIEW OF MULTIRATE OUTPUT FEEDBACK BASED DISCRETE TIME SLIDING MODE CONTROL (USING BARTOSZEWICZ LAW) [64]

The theory of sliding model control (SMC) is based on the concept of varying the structure of the controller by changing state of the system in order to obtain a desired response [52]. Generally, a switching control action is used to switch between different structures and the system state is forced to move along the chosen manifold, called the switching manifold which determines the closed loop system behavior [53], [54]. In the recent years, considerable efforts have been put into studying the concepts of Digital Sliding Mode (DSM) controller design [55]-[57].

In the case of DSM design, the control input is applicable only at certain sampling instants and the control effort remains constant over the entire sampling period. Moreover, when the states reach the switching surface, the subsequent control would be unable to keep the states confined to the surface. As a result, DSM can undergo only quasi-sliding mode, i.e., the system states would approach the sliding surface but would generally be unable to stay on it. Thus, in general, DSM does not possess the invariance property found in CT sliding mode.

Bartoszewicz [58] proposed a state feedback based control law for uncertain systems that guarantees discrete sliding mode. Moreover, this law avoids the switching function present in other sliding mode control algorithms such as in [57] and thus avoids chatter. However, the above-mentioned sliding mode control strategies require full-state feedback. But, in practice, all the states of the system are not always available for measurement. Since the system output is always available for measurement, output feedback [18], [43] can be used for controller design.

The problem of static output feedback [50] is a well-researched one. However, no results are available till today which show that guaranteed closed loop stability [23] can be achieved by using static output feedback [37]. The guaranteed stability of the closed loop system can be achieved by using fast output sampling technique [47], [59]. Werner in [59] has used fast output sampling (FOS) feedback which has the features of static output feedback [29] and makes it possible to arbitrarily assign the closed loop poles of the system. Unlike static output feedback, fast output sampling feedback [46] always guarantees the stability of the closed loop system.

In fast output sampling [46], each sampling period  $\tau$  is subdivided into  $N$  subintervals of width  $\Delta = \tau / N$ .  $N$  must be chosen to be greater than or equal to the observability index of the system. The last  $N$  output samples are measured at time instants  $t = l\Delta$ ,  $l = 0, 1, 2, \dots$  and a constant control signal  $u$  is applied over a period  $\tau$ . The control signal is constructed as a linear combination of the last  $N$  output samples.

In this paper, the discrete-time multirate output feedback sliding mode control algorithm proposed in [60] that is based on Bartoszewicz's control law [58] and fast output sampling feedback [59] is used for systems with disturbance (impulse). Here, the disturbance is the external force signal  $r(t)$ , which is applied to the beam at its free end. This algorithm has the advantage that it does not require the state information for control purpose. The control input is deduced using past output samples and the immediate past input signal alone. Moreover, the strategy used here eliminates the restriction on the closed loop system poles not being at the origin as imposed in [59].

Consider a discrete-time  $n^{\text{th}}$  order single output system that is sampled with a sampling interval  $\tau$  sec.

$$\begin{aligned} x(k+1) &= \Phi_{\tau}x(k) + \Delta\Phi_{\tau}x(k) + \Gamma_{\tau}u(k) + f(k), \\ y(k) &= Cx(k), \end{aligned} \quad (86)$$

here,  $\Delta\Phi_{\tau}$  is the uncertainty in the state,  $f(k)$  is an external disturbance vector and  $(\Phi_{\tau}, \Gamma_{\tau}, C)$  are matrices of appropriate dimensions with  $(\Phi_{\tau}, \Gamma_{\tau})$  being controllable and  $(\Phi_{\tau}, C)$  being observable. Let us define the disturbance vector as

Let us define the disturbance vector as

$$\tilde{d}(k) = \Delta\Phi_{\tau}x(k) + f(k). \quad (87)$$

Let the desired sliding manifold be governed by the parameter vector  $c^T$  such that  $c^T\Gamma_{\tau} \neq 0$  and the resulting quasi-sliding motion is stable and let the disturbance be bounded such that

$$d(k) = c^T\tilde{d}(k) \quad (88)$$

satisfies the inequality

$$d_l \leq d(k) \leq d_u, \quad (89)$$

where  $d_l$  and  $d_u$  are the known upper and lower bounds on the disturbance respectively. Here, we define the following terms

$$d_0 = 0.5(d_l + d_u), \quad \delta_d = 0.5(d_u - d_l), \quad (90)$$

The switching surface is given by

$$s(k) = c^T x(k). \quad (91)$$

The quasi-sliding mode is defined as the motion such that  $|s(k)| \leq \varepsilon$ , where the positive constant  $\varepsilon$  is called the quasi-sliding-mode bandwidth. A reaching law proposed by Bartoszewicz [58] is of the form

$$s(k+1) = d(k) - d_0 + s_d(k+1), \quad (92)$$

where  $d(k)$  is defined in Eq. (89) and  $s_d(k)$  is a priori known function that satisfies the following conditions.

a. If  $|s(0)| > 2\delta_d$ , then  $s_d(0) = s(0)$ ,

$$s_d(k)s_d(0) \geq 0 \text{ for any } k \geq 0,$$

$$s_d(k) = 0 \text{ for any } k \geq k^*,$$

$$|s_d(k+1)| < |s_d(k)| - 2\delta_d, \text{ for any } k < k^*.$$

b. If  $|s(0)| \leq 2\delta_d$  then,

$$s_d(k) = 0 \text{ for any } k \geq 0. \quad (94)$$

The value of the positive integer  $k^*$  is chosen by the designer so as to have a trade off between faster convergence and the magnitude of the control input  $u$ . By controlling the rate of decay (tuning  $k^*$ ), the convergence of  $s(k) = 0$  is tuned. The reaching law in Eq. (92) together with the 2 conditions of the function  $s_d(k)$  imply that the reach law condition is satisfied and that, for any  $k \geq k^*$ , the QSM in the  $\delta_d$  vicinity of the sliding plane  $s(k) = c^T x(k) = 0$  exists. One possible function for  $s_d(k)$ , when  $|s(0)| \geq 2\delta_d$  can be described as

$$s_d(k) = \frac{(k^* - k)}{k^*} s(0), \quad k = 0, 1, \dots, k^*, \quad (95)$$

where

$$k^* < \frac{|s(0)|}{2\delta_d}. \quad (96)$$

The control law that satisfies the reaching law defined in (92) and achieves sliding mode for the system with disturbance described in (86), can be computed to be

$$u(k) = -\left(c^T \Gamma_\tau\right)^{-1} \left(c^T \Phi_\tau x(k) + d_0 - s_d(k+1)\right). \quad (97)$$

When the control input described in (97) is fed into the system, it would guarantee that for any  $k \geq k^*$ , the system would satisfy the inequality

$$|s(k)| = |d(k-1) - d_0| \leq \delta_d. \quad (98)$$

Hence, the states of the system settle within a quasi-sliding mode band whose width is less than half the width of the band described in [57].

In [60], a multirate output feedback based equivalent of the above algorithm was proposed using a modified reaching law as

$$s(k+1) = d(k) - d_0 + e(k-1) - e_0 + s_d(k+1), \quad (99)$$

where a new variable  $e(k)$  is introduced. The control input generated using this algorithm [60] can be represented as

$$u(k) = -\left(c^T \Gamma_\tau\right)^{-1} \left(c^T \Phi_\tau L_y y_k + c^T \Phi_\tau L_u u(k-1) + d_0 + e_0 - s_d(k+1)\right), \quad (100)$$

where,

$$L_y = \Phi_\tau C_0^{-1}, L_u = \Gamma_\tau - C_0^{-1} D_0, L_d = I - C_0^{-1} C_d, \quad (101)$$

$$C_0 = \begin{bmatrix} C \\ C\Phi \\ C\Phi^2 \\ \vdots \\ C\Phi^{N-1} \end{bmatrix}, D_0 = \begin{bmatrix} 0 \\ C\Gamma \\ C(\Phi\Gamma + \Gamma) \\ \vdots \\ C \sum_{i=0}^{N-2} \Phi^i \Gamma \end{bmatrix}, \quad (102)$$

$$C_d = \begin{bmatrix} 0 \\ C \left( \sum_{i=0}^{N-1} \Phi^i \right)^{-1} \\ C \left( \sum_{i=0}^1 \Phi^i \right) \left( \sum_{i=0}^{N-1} \Phi^i \right)^{-1} \\ \vdots \\ C \left( \sum_{i=0}^{N-2} \Phi^i \right) \left( \sum_{i=0}^{N-1} \Phi^i \right)^{-1} \end{bmatrix}, \quad (103)$$

$e_0 = 0.5(e_l + e_u)$  and  $\delta_e = 0.5(e_u - e_l)$  are the mean (average value) and the variation (maximum deviation) of the function of the uncertainty.  $e_l$  and  $e_u$  are the lower and upper bounds of  $e(k)$ . The new variable  $e(k)$ , which is the effect of disturbance on the sampled output is defined as

$$e(k) = c^T \Phi_\tau L_d \tilde{d}(k) \quad (104)$$

where the bounds on  $e(k)$  is given by  $e_l \leq e(k) \leq e_u$ , since the disturbance  $\tilde{d}(k)$  is bounded. The value of  $N$  is chosen to be  $>$  the observability index  $\nu$  of the system defined as “the observability index of a system represented by the triplet

$(A, B, C)$  is the minimum integer value of  $\nu$  such that”

$$\text{Rank} \begin{bmatrix} C \\ CA \\ \vdots \\ CA^{\nu-1} \end{bmatrix} = \text{Rank} \begin{bmatrix} C \\ CA \\ \vdots \\ CA^\nu \end{bmatrix} \quad (105)$$

Hence, the control input can be computed using the past output samples and the immediate past input signal. But, at  $k=0$ , there are no past outputs for use in control, hence  $u(0)$  is obtained by ignoring  $e(k-1)$  and  $e_0$  (as we expect no disturbance before the instant  $k=0$  to affect the system) and assuming an initial state  $x(0)$  to obtain

$$s(k+1) = d(k) - d_0 + e(k-1) - e_0 + s_d(k+1), \quad (106)$$

$$s(k) = d(k-1) - d_0 + e(k-2) - e_0 + s_d(k). \quad (107)$$

When  $k > \max(k^*, 2)$ ,  $s_d(k) = 0$  and therefore

$$s(k) = d(k-1) - d_0 + e(k-2) - e_0. \quad (108)$$

Thus, we have

$$|s(k)| = |d(k-1) - d_0 + e(k-2) - e_0| \leq |d(k-1) - d_0| + |e(k-2) - e_0| = \delta_d + \delta_e, \quad (109)$$

$$|s(k)| \leq \delta_d + \delta_e.$$

It can be seen that this algorithm does not need the measurement of the states of the system for the generation of the control input. But, as a trade off, the width of the quasi-sliding mode band is increased by  $\delta_e$ . The control technique discussed in the previous paragraphs [60] is used to design a MROF based DSMC control scheme to suppress the vibrations in a smart structure, which is modeled using Timoshenko beam theory for 2 vibratory modes.

#### IV. DESIGN OF DISCRETE SLIDING MODE CONTROLLER USING MULTIRATE OUTPUT FEEDBACK TECHNIQUE

The control technique discussed in the previous section [60] is used to design a controller to suppress the first 2 vibration modes of a flexible cantilever beam through smart structure concept for the various SISO state space models of the smart beam given in section 2 in Eqs. (82)-(85) in which the piezo patches are placed at various locations [61], [62].

The first task in designing the DSMC controller is the selection of the sampling interval  $\tau$ . The maximum bandwidth for all the sensor / actuator locations on the beam are calculated (here, the 2<sup>nd</sup> vibratory mode of the plant) and then by using existing empirical rules for selecting the sampling interval based on bandwidth, approximately 10 times of the maximum 2<sup>nd</sup> vibration mode frequency of the system has been selected. The sampling interval used is  $\tau = 0.004$  seconds [63].

The cantilever beam is divided into 4 finite elements. PZT's are bonded to the beam at one FE position only as a collocated pair, say, at fixed end (FE location 1) or at FE position 2 or at FE position 3 or at FE position 4 (free end), thus giving rise to

4 SISO models (1 actuator input  $u$  and 1 sensor output  $y$ ) of the same smart structure plant as shown in the Fig. 2.

The beam is excited by an impulse signal applied at the free end of it as shown in the Fig. 2. The beam is thus subjected to vibrations and the open loop impulse response (plot of sensor outputs  $y$  as a function of  $t$  of the various SISO models are observed without the controller. The designed DSMC controller is put in loop with the plant and the closed loop responses, the control input and the sliding function are observed for all the 4 SISO models of the same smart structure plant. The performance of these 4 SISO models is evaluated for AVC by carrying out the simulations in MATLAB, observing the various responses and finally concluding with the discussions on the simulation results. The frequency response plots of the 4 models are also observed.

V. SIMULATION RESULTS

The application of the control law [60] to the SISO smart structure model derived in Section 3 gave the following simulation results shown in the Figs. 3 - 18.

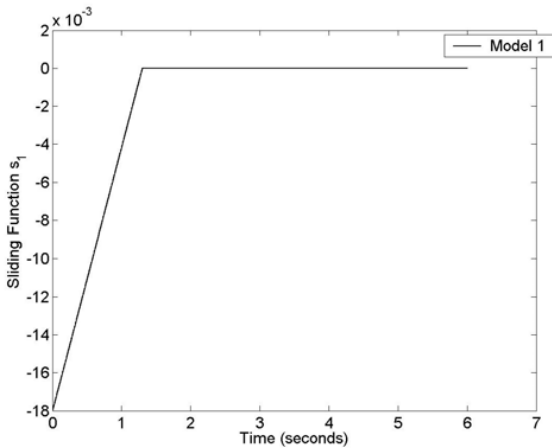


Fig. 3 Plot of sliding function for model 1 (PZT) at FE 1

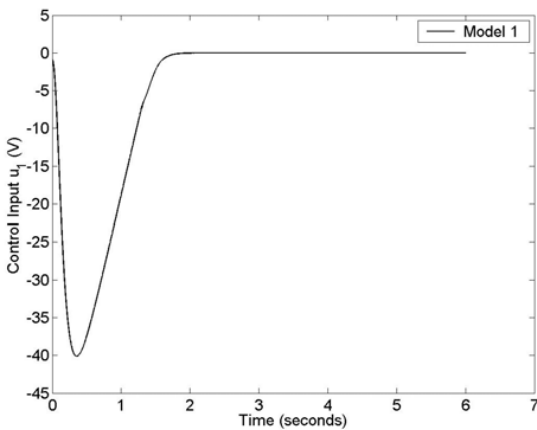


Fig. 4 Plot of control effort for model 1 (PZT) at FE 1

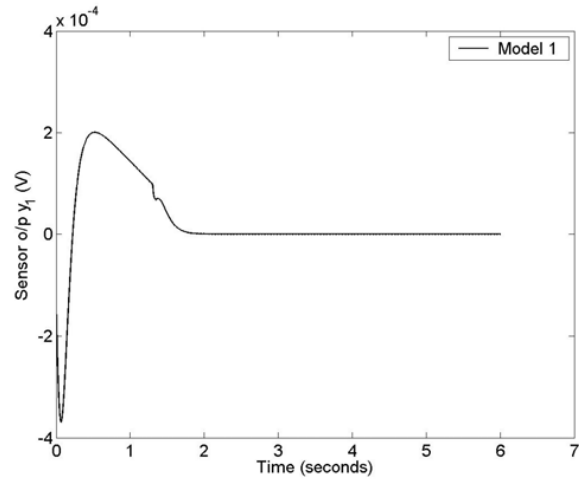


Fig. 5 Plot of sensor output for model 1 (PZT) at FE 1

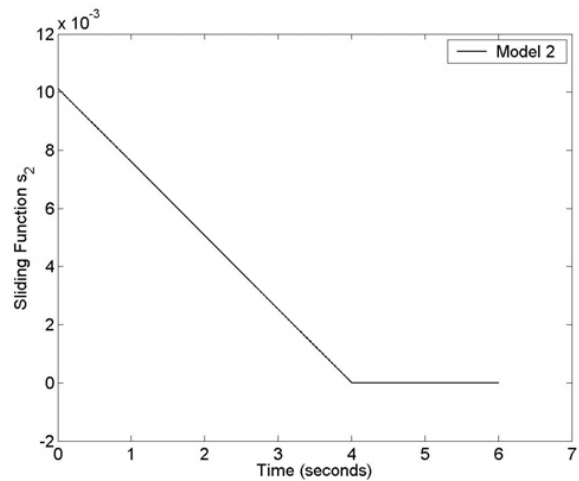


Fig. 6 Plot of sliding function for model 2 (PZT) at FE 2

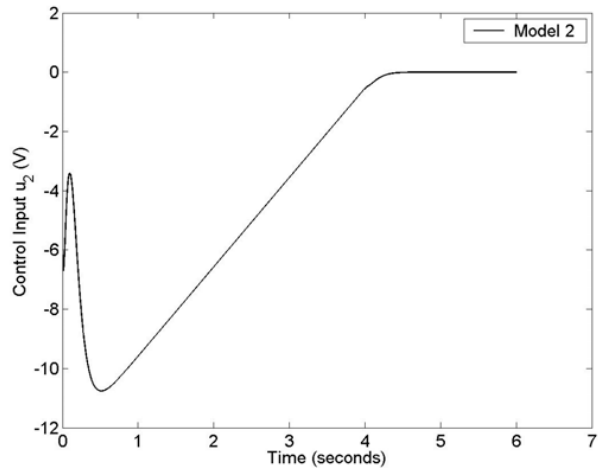


Fig. 7 Plot of control effort for model 2 (PZT) at FE 2

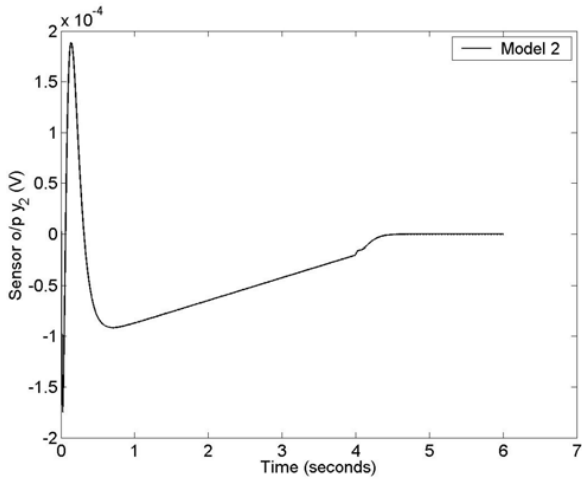


Fig. 8 Plot of sensor output for model 2 (PZT) at FE 2

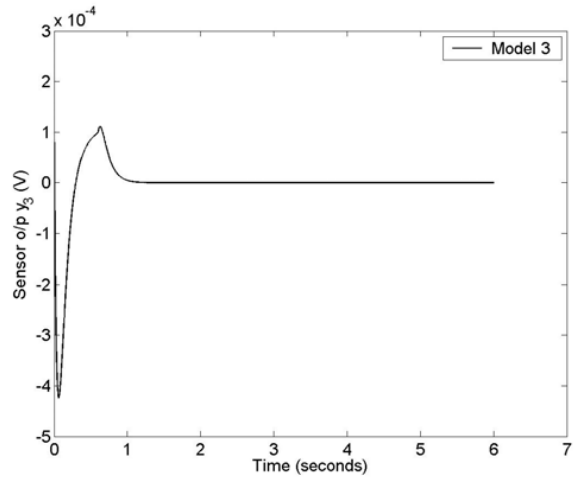


Fig. 11 Plot of sensor output for model 3 (PZT) at FE 3

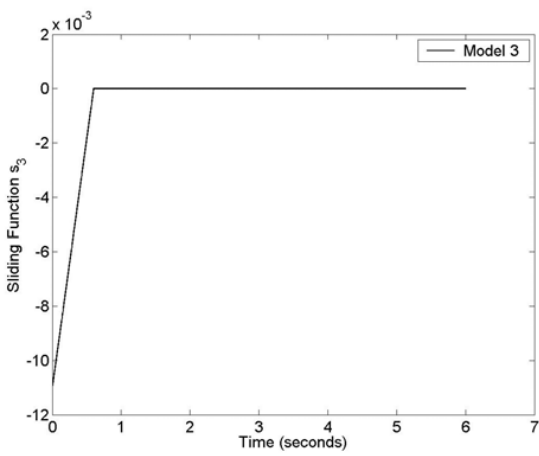


Fig. 9 Plot of sliding function for model 3 (PZT) at FE 3

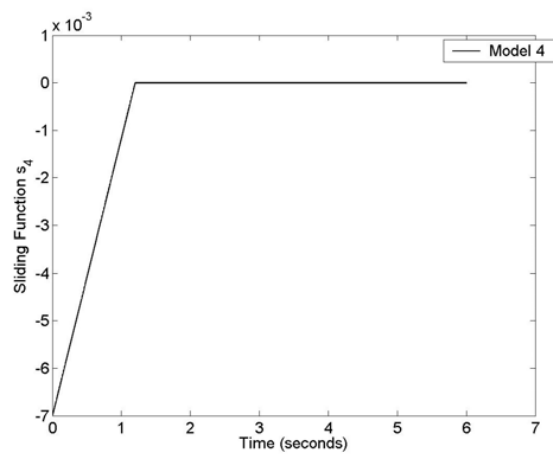


Fig. 12 Plot of sliding function for model 4 (PZT) at FE 4

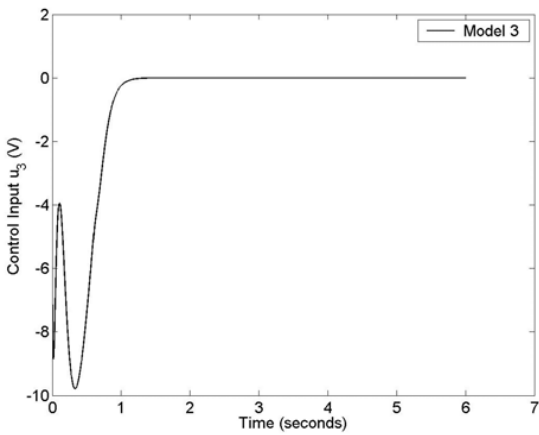


Fig. 10 Plot of control effort for model 3 (PZT) at FE 3

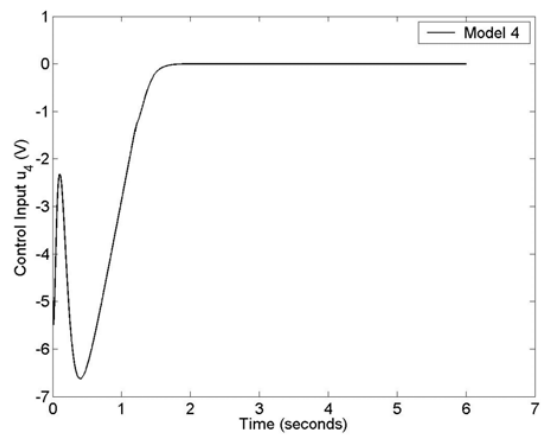


Fig. 13 Plot of control effort for model 4 (PZT) at FE 4

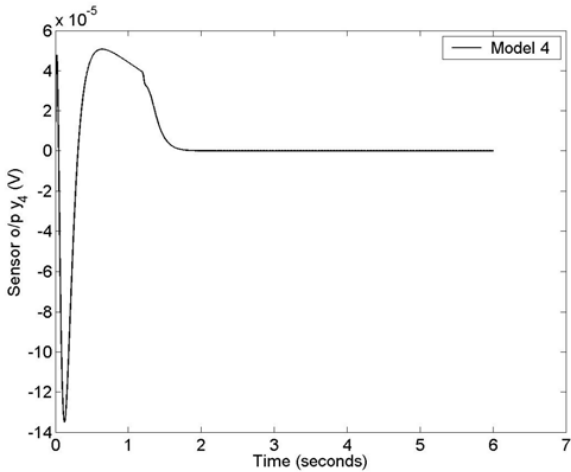


Fig. 14 Plot of sensor output for model 4 (PZT) at FE 4

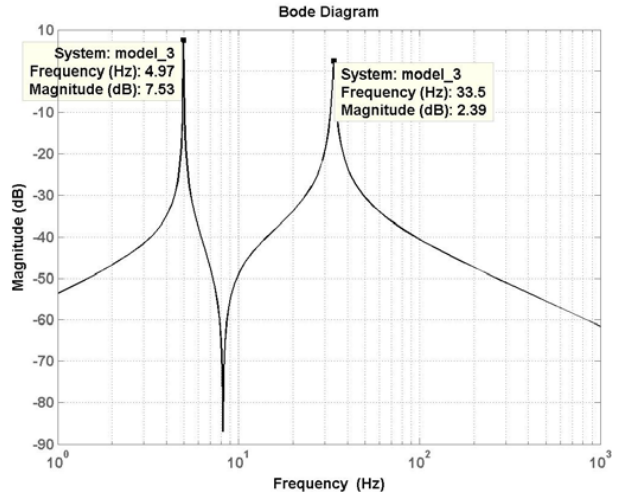


Fig. 17 Bode plot for model 3

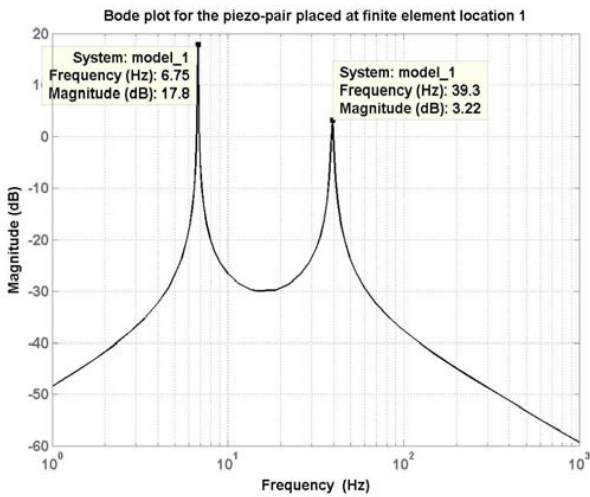


Fig. 15 Bode plot for model 1

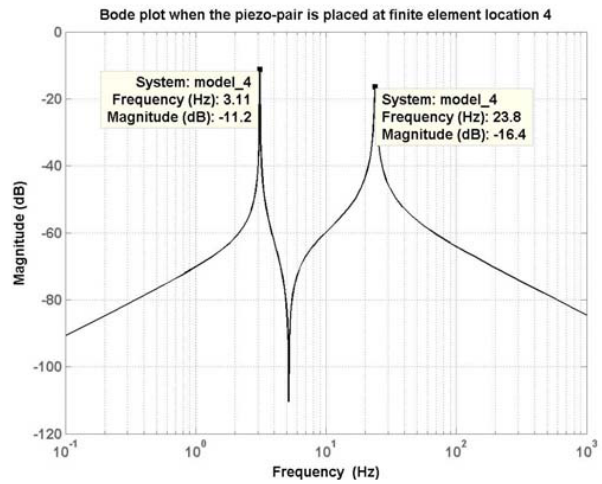


Fig. 18 Bode plot for model 4

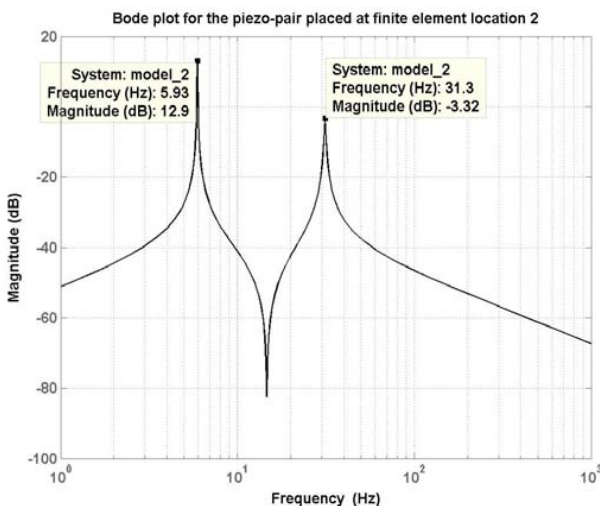


Fig. 16 Bode plot for model 2

## VI. CONCLUSION

An application of the discrete time sliding mode control proposed in [60] is used for the design of controllers for smart structure vibration control in this paper. Here, the comparison and discussion of the simulation results of the vibration control for the smallest magnitude of the control effort  $u$  required to control the vibrations of the smart cantilever beam is presented. The best model for AVC is also arrived at. From the simulation results, it is observed that

- Modeling a smart structure by including the sensor / actuator mass and stiffness and by varying its location on the beam from the free end to the fixed end introduces a considerable change in the system's structural vibration characteristics,
- The uncontrolled system takes much longer time to damp out the oscillations as compared to the system with the designed sliding mode control input, i.e., without control the transient response was predominant and with control, the vibrations are suppressed,

- When the piezo element is placed near the root, the sensor output voltage is greater because of the heavy distribution of the bending moment near the fixed end, thus leading to a larger strain rate,
- Sensor voltage is less when the piezo pair is located at the free end because of lesser strain rate and hence require more control effort,
- Sensitivity of the sensor / actuator pair depends on its location on the beam from the root hub, collocation of the piezo pair and the gain of the amplifier used,
- System responds well in CL and does not exhibit undesirable chattering phenomenon. Neither does the system vibrate much,
- MROF based DSMC avoids the use of the signum function in the control input and the control law uses only the past output samples and the past control input instead of the system states, guarantees faster convergence of the system,
- Representative point to the QSM band around the line  $c^T x(k) = 0$  and better steady state accuracy of the control system,
- Comparing the 4 SISO models, it is observed that as the smart beam is divided into 4 FE with piezo pair at the fixed end (SISO model 1), the vibration characteristics are the best to demonstrate the AVC of smart beams because of the above-mentioned inferences.

Hence, it may be concluded that an effective vibration control technique is demonstrated here. The limitations of Euler-Bernoulli beam theory such as the neglect of the shear and axial displacements have been considered here. Thus, the Timoshenko beam theory corrects the simplifying assumptions made in Euler-Bernoulli beam theory and the model obtained can be closer to a exact one.

## ACRONYMS

FOS	Fast Output Sampling
SISO	Single Input Single Output
MIMO	Multi Input Multi Output
FEM	Finite Element Method
FE	Finite Element
LMI	Linear Matrix Inequalities
MR	Magneto Rheological
ER	Electro Rheological
PVDF	Poly Vinylidene Fluoride
CF	Clamped Free
CC	Clamped Clamped
CT	Continuous Time
DT	Discrete Time
HOBT	Higher Order Beam Theory
DTSMC	Discrete Time Sliding Mode Control
SMC	Sliding Mode Control
MROF	Multi-Rate Output Feedback
RHS	Right Hand Side
LTI	Linear Time Invariant
EB	Euler-Bernoulli

PZT	Lead Zirconate Titanate
IEEE	Institute of Electrical & Electronics Engineers
IOP	Institute of Physics
ISSS	Institute of Smart Structures and Systems
SPIE	Society of Photonics & Instrumentation Engineers

## NOMENCLATURE

$f_{ext}$	External force input
$l$	Length of the beam
$b$	Width of the beam
$E_b$	Young's modulus of beam
$\rho, \rho_b$	Mass density of beam
$\alpha, \beta$	Structural constants
$t_b$	Thickness of beam
$l_p$	Length of the piezoelectric patch
$t_a$	Thickness of actuator
$t_s$	Thickness of sensor
$E_p$	Young's modulus of piezoelectric
$\rho_p$	Mass density of piezoelectric
$d_{31}$	Piezoelectric strain constant
$g_{31}$	Piezoelectric stress constant
$\theta$	Bending angle (rotation about $Y$ axis)
$\beta$	Shear angle
$X, Y$ and $Z$	The 3 axis of 3D space
$u$	Axial displacement along $X$ axis
$v$	Lateral displacement along the $Y$ axis
$T, U$	Kinetic energy and strain energy
$\sigma_{xz}, \sigma_{xx}$	Shear stress, Tensile stress
$K = \frac{G}{2}$	Shear coefficient
$\varepsilon$	Linear strain
$\gamma$	Shear strain
$I$	Mass MI of beam element
$A$	Area of cross section of beam element
$\dot{w}$	Linear velocity
$q_d$	Distributed force along length of the beam
$m$	Moment along the length of the beam
$W_e$	Work done due to the external forces
$W$	External work done
$t$	Time in secs
$a_i$	Unknown coefficients ( $i=1, 2, 3, 4$ )
$b_j$	Unknown coefficients ( $j=1, 2, 3$ )
$\mathbf{q}$	Vector of displacements and slopes
$\dot{\mathbf{q}}$	Strain rate
$E_f$	Electric field



$D$	Dielectric displacement	$K^b$	Stiffness matrix of the regular beam element (also called as the local stiffness matrix)
$e$	Permittivity of the medium	$M^b$	Mass matrix of the regular beam element (also called as the local Mass matrix)
$s^E$	Compliance of the medium	$[M_{\rho A}]$	Mass matrix associated with translational inertia
$d$	Piezoelectric constant	$\epsilon_{xx}, \epsilon_{yy}, \epsilon_{zz}$	Longitudinal strains or the tensile strains in the 3 directions
$Q(t)$	Charge developed on the sensor surface	$\gamma_{xz}, \gamma_{yz}, \gamma_{xy}$	Shear strains induced in the beam along the 3 directions
$i(t)$	Current generated by the sensor surface	$G$	Shear modulus (or modulus of rigidity) of the beam
$e_{31}$	Piezoelectric stress / charge constant	$\Phi_\tau, \Gamma_\tau$	System matrix, input matrix discretized at sampling interval of $\tau$ secs
$V^s$	Sensor voltage $V^s$	$\Phi, \Gamma$	System matrix, input matrix discretized at sampling interval of $\Delta$ secs
$G_c$	Signal-conditioning device with gain	<b>A, B, C, D</b>	State space matrices (CT) : System matrix, input matrix, output matrix, transmission matrix
$K_c$	Controller gain $K_c$	<b>E</b>	External load matrix which couples the disturbance to the system
$y(t)$	Output of the system (sensor output)	<b>M, K</b>	Mass and stiffness of the regular beam element
$V^a(t)$	Actuator voltage	$\mathbf{p}^T$	Constant vector, which depends on sensor characteristics
$V^s(t)$	Sensor voltage	$\mathbf{h}^T$	Constant vector, which depends on actuator characteristics
$\mathbf{f}_{ctrl}$	Control force applied by the actuator	$w$	Time dependent transverse displacement of $Z$ axis
$\mathbf{f}^t$	Total force coefficient vector	$M_A$	Resultant moment acting on the beam because of electric field
$\mathbf{M}^*$	Generalized mass matrix	<b>M</b>	Assembled mass matrices (global mass matrix)
$\mathbf{K}^*$	Generalized stiffness matrix	<b>K</b>	Assembled stiffness matrices (global stiffness matrix), Periodic output feedback gain
$\mathbf{C}^*$	Generalized damping matrix	<b>T</b>	Modal matrix containing the eigenvectors representing the 1 <sup>st</sup> 2 modes
$\mathbf{g}$	Principal coordinates	$\mathbf{f}_{ext}^*$ and $\mathbf{f}_{ctrl}^*$	Generalized external force vector and generalized control force vector
$u(t)$	Control input		
$r(t)$	External input to the system		
$x(t)$	State vector		
$\dot{x}(t)$	Derivative of the state vector		
$\mathfrak{R}^n$	$n$ dimension space		
$\tau$	Sampling interval		
$G$	Output injection gain		
$v$	Controllability index of the system		
$u_k, y_k$	Input and output at the $k^{th}$ instant		
$\mathbf{C}_0, \mathbf{D}_0$	Lifted system matrices		
$\rho_1, \rho_2, \rho_3$	Spectral norms		
$I$	Identity matrix		
$N$	Number of sub-intervals		
$L$	Length of beam element		
$M^p$	Mass matrix of the piezoelectric element		
$A_p$	Area of the piezoelectric patch		
$[M_{\rho I}]$	Mass matrix with rotary inertia		
$K^p$	Stiffness matrix of piezoelectric element		
$\phi$	Ratio of beam bending stiffness to shear stiffness		
$[N_w]^T$	Mode shape functions for displacement taking $\phi$ into consideration		
$[N_\theta]^T$	Mode shape functions for rotations taking $\phi$ into consideration		
$[N_a]^T$	Mode shape functions for accelerations taking $\phi$ into consideration		

## REFERENCES

- [1] H. Abramovich, and A. Lishvits, "Free vibrations of non-symmetric cross-ply laminated composite beams," *Journal of Sound and Vibration*, vol. 176, no. 5, pp. 597 - 612, 1994.
- [2] O. J. Aldraihem, R. C. Wetherhold, and T. Singh, "Distributed control of laminated beams : Timoshenko Vs. Euler-Bernoulli Theory," *J. of Intelligent Materials Systems and Structures*, vol. 8, pp. 149-157, 1997.
- [3] H. Abramovich, "Deflection control of laminated composite beam with piezoceramic layers-Closed form solutions," *Composite Structures*, vol. 43, no. 3, pp. 217-131, 1998.
- [4] O. J. Aldraihem, and K. A. Ahmed, "Smart beams with extension and thickness-shear piezoelectric actuators," *Smart Materials and Structures*, vol. 9, no. 1, pp. 1-9, 2000.
- [5] A. K. Ahmed, and J. A. Osama, "Deflection analysis of beams with extension and shear piezoelectric patches using discontinuity functions" *Smart Materials and Structures*, vol. 10, no. 1, pp. 212-220, 2001.
- [6] L. E. Azulay, and H. Abramovich, "Piezoelectric actuation and sensing mechanisms-Closed form solutions," *Composite Structures J.*, vol. 64, pp. 443-453, 2004.

- [7] T. Baily, and J. E. Hubbard Jr., "Distributed piezoelectric polymer active vibration control of a cantilever beam," *J. of Guidance, Control and Dynamics*, vol. 8, no.5, pp. 605-611, 1985.
- [8] M. J. Balas, "Feedback control of flexible structures," *IEEE Trans. Automat. Contr.*, vol. AC-23, no. 4, pp. 673-679, 1978.
- [9] J. S. Burdess, and J. N. Fawcett, "Experimental evaluation of piezoelectric actuator for the control of vibrations in a cantilever beam," *J. Syst. Control. Engg.*, vol. 206, no. 12, pp. 99-106, 1992.
- [10] M. J. Brennan, J. G. Bonito, S. J. Elliot, A. David, and R.J. Pinnington, "Experimental investigation of different actuator technologies for active vibration control," *Journal of Smart Materials and Structures*, vol. 8, pp. 145-153, 1999.
- [11] B. M. Bona, M. Indri, and A. Tornamble, "Flexible piezoelectric structures-approximate motion equations and control algorithms," *IEEE Trans. on Auto. Contr.*, vol. 42, no. 1, pp. 94-101, 1997.
- [12] A. Benjeddou, M. A. Trindade, and R. Ohayon, "New shear actuated smart structure beam finite element," *AIAA J.*, vol. 37, pp. 378-383, 1999.
- [13] E. F. Crawley, and J. De Luis, "Use of piezoelectric actuators as elements of intelligent structures," *AIAA J.*, vol. 25, pp. 1373-1385, 1987.
- [14] K. Chandrashekhara, and S. Varadarajan, "Adaptive shape control of composite beams with piezoelectric actuators," *J. of Intelligent Materials Systems and Structures*, vol. 8, pp. 112-124, 1997.
- [15] B. Culshaw, "Smart Structures : A concept or a reality," *J. of Systems and Control Engg.*, vol. 26, no. 206, pp. 1-8, 1992.
- [16] C. R. Cooper, "Shear coefficient in Timoshenko beam theory," *ASME J. of Applied Mechanics*, vol. 33, pp. 335-340, 1966.
- [17] S. B. Choi, C. Cheong, and S. Kini, "Control of flexible structures by distributed piezo-film actuators and sensors," *J. of Intelligent Materials and Structures*, vol. 16, pp. 430-435, 1995.
- [18] A. B. Chammas, and C. T. Leondes, "Pole placement by piecewise constant output feedback," *Int. J. Contr.*, vol. 29, pp. 31-38, 1979.
- [19] C. Doschner, and M. Enzmann, "On model based controller design for smart structure," *Smart Mechanical Systems Adaptronics SAE International USA*, pp. 157-166, 1998.
- [20] P. Donthireddy, and K. Chandrashekhara, "Modeling and shape control of composite beam with embedded piezoelectric actuators," *Comp. Structures*, vol. 35, no. 2, pp. 237-244, 1996.
- [21] J. L. Fanson, and T. K. Caughey, "Positive position feedback control for structures," *AIAA J.*, vol. 18, no. 4, pp. 717-723, 1990.
- [22] P. Forouza, "Distributed controllers for flexible structures using piezoelectric actuators / sensors," *Proc. the 32<sup>nd</sup> Conference on Decision and Control, Texas*, pp. 1367-1369, Dec. 1993.
- [23] J. C. Geromel, C. C. De Souza, and R. E. Skeleton, "LMI Numerical solution for output feedback stabilization," *Proc. American Contr. Conf.*, pp. 40-44, 1994.
- [24] S. V. Gosavi, and A. V. Kelkar, "Modeling, identification, and passivity-based robust control of piezo-actuated flexible beam," *Journal of Vibration and Acoustics*, vol. 129, pp. 260-271, Apr. 2004.
- [25] P. Gahinet, A. Nemirovski, A. J. Laub, and M. Chilali, "LMI Tool box for Matlab", *The Math works Inc., Natick MA*, 1995.
- [26] S. Hanagud, M. W. Obal, and A. J. Callise, "Optimal vibration control by the use of piezoceramic sensors and actuators," *J. of Guidance, Control and Dyn.*, vol. 15, no. 5, pp. 1199-1206, 1992.
- [27] W. Hwang, and H. C. Park, "Finite element modeling of piezoelectric sensors and actuators", *AIAA J.*, vol. 31, no. 5, pp. 930-937, 1993.
- [28] J. B. Kosmatka, and Z. Friedman, "An improved two-node Timoshenko beam finite element", *Computers and Struct.*, vol. 47, no. 3, pp. 473-481, 1993.
- [29] W. S. Levine, and M. Athans, "On the determination of the optimal constant output feedback gains for linear multivariable systems," *IEEE Trans. Auto. Contr.*, vol. AC-15, pp. 44-48, 1970.
- [30] T. C. Manjunath and B. Bandyopadhyay, "Modeling and fast output sampling feedback control of a smart Timoshenko cantilever beam," *International Journal of Smart Structures and Systems*, Vol. 1, no. 3, pp. 283-308, Sep. 2005.
- [31] G. Murali, G.A. Pajunen, "Model reference control of vibrations in flexible smart structures," *Proc. 34<sup>th</sup> Conference on Decision and Control, New Orleans, USA*, pp. 3551-3556, Dec. 1995.
- [32] J. S. M. Moita, I. F. P. Coreia, C. M. M. Soares, and C. A. M. Soares, "Active control of adaptive laminated structures with bonded piezoelectric sensors and actuators," *Computers and Structures*, vol. 82, pp. 1349 - 1358, 2004.
- [33] Robin Scott, Michael Brown and Martin Levesley, "Robust multivariable control of a double beam cantilever smart structure," *J. of Smart Materials and Structures*, vol. 13, pp. 731-743, 2003.
- [34] S. Raja, G. Prathap, and P. K. Sinha, P.K., "Active vibration control of composite sandwich beams with piezoelectric extension-bending and shear actuators," *Smart Materials and Structures*, vol. 11, no. 1, pp. 63-71, 2002.
- [35] S. Rao, and M. Sunar, "Piezoelectricity and its uses in disturbance sensing and control of flexible structures : A Survey," *Applied Mechanics Rev.*, vol. 47, no. 2, pp. 113-119, 1994.
- [36] C. T. Sun, and X. D. Zhang, "Use of thickness-shear mode in adaptive sandwich structures," *Smart Materials and Structures J.*, vol. 3, no. 4, pp. 202-206, 1995.
- [37] V. L. Syrmos, P. Abdallah, P. Dorato, and K. Grigoriadis, "Static output feedback : A survey," *Automatica*, vol. 33, no. 2, pp. 125-137, 1997.
- [38] W. Schiehlen, and H. Schonerstedt, "Controller design for the active vibration damping of beam structure," *Smart Mechanical Systems Adaptronics SAE International, USA*, pp. 137-146, 1998.
- [39] P. Seshu, "Textbook of Finite Element Analysis," 1st Ed. Prentice Hall of India, New Delhi, 2004.
- [40] W. Shiang Lee, "System identification and control of smart structures using neural networks," *Automatica*, vol. 38, no. 4-8, pp. 269-276, 1996.
- [41] J. Thomas, and B. A. H. Abbas, "Finite Element Methods for dynamic analysis of Timoshenko beam," *J. of Sound and Vibration*, vol. 41, pp. 291-299, 1975.
- [42] M. O. Tokhi, "Self tuning active vibration control in flexible beam structures," *Journal of Systems and Control Engineering - Proceedings of the Institute of Mechanical Engineers*, vol. 208, pp. 263-277, 1994.
- [43] H. Werner, "Robust multivariable control of a turbo-generator by periodic output feedback," vol. 31, no. 4, pp. 395 - 411, 1997.
- [44] Ulrich Gabbertl, Tamara Nestorović Trajkovi, and Heinz Köppel, "Modeling, control and simulation of piezoelectric smart structures using finite element method and optimal LQ control," *Facta Universitatis Series: Mechanics, Automatic Control and Robotics*, Vol. 3, no. 12, pp. 417 - 430, 2002.
- [45] Vukovich, G., and A.Y. Koma. Vibration suppression of flexible beams with bonded piezo-transducers using wave-absorbing controllers in *J. Guidance, Control and Dynamics*, pp. 347-354, Mar-Apr. 2000.
- [46] H. Werner, and K. Furuta, "Simultaneous stabilization based on output measurements," *Kybernetika*, vol. 31, no. 4, pp. 395-411, 1995.
- [47] H. Werner, H., "Multimodal robust control by fast output sampling-An LMI approach," *Automatica*, vol. 34, no. 12, pp. 1625-1630, 1998.
- [48] Young-Hun Lim, V. Senthil Gopinathan, Vasundara V Varadhan, and K. Vijay K Varadan, "Finite element simulation of smart structures using an optimal output feedback controller for vibration and noise control," *Journal of Smart Materials and Structures*, vol. 8, pp. 324-337, 1999.
- [49] S. M. Yang, and Y. J. Lee, "Optimization of non-located sensor / actuator location and feedback gain in control systems," *Journal of Smart Materials Structures*, vol. 8, pp. 96-102, 1993.
- [50] Y. C. Yan, J. Lam, and Y. X. Sun, "Static output feedback stabilization: An LMI approach," *Automatica*, vol. 34, no. 12, pp. 1641-1645, 1998.
- [51] X. D. Zhang, and C. T. Sun, "Formulation of an adaptive sandwich beam," *Smart Mater. and Struct.*, vol. 5, no.6, pp. 814-823, 1996.
- [52] V.I. Utkin, "Variable structure systems with sliding modes", *IEEE Trans. Automat. Contr.*, vol. AC-22, pp. 212-222, 1977.
- [53] J.Y. Hung, W. Gao, and J.C. Hung, "Variable structure control : A survey", *IEEE Trans. Ind. Electron.*, Vol. 40, no. 1, pp. 2-21, 1993.
- [54] K.D. Young, V.I. Utkin, U. Ozguner, "A control engineer's guide to sliding mode control", *IEEE Trans. Contr. Syst.*, vol. 7, no. 3, pp. 328-342, 1999.
- [55] S. Sarpurk, Y. Istefanopoulos, and O. Kaynak, "On the stability of discrete-time sliding mode systems", *IEEE Trans. Automat. Contr.*, vol. AC-32, pp. 930-932, 1987.
- [56] K. Furuta, "Sliding mode control of a discrete system", *Syst. Control Lett.*, vol. 14, pp. 145-152., 1990.
- [57] W. Gao, Y. Wang, and A. Homaifa, "Discrete-time variable structure control systems," *IEEE Trans. Ind. Electron.*, vol. 42, pp. 117-122, 1995.
- [58] A. Bartoszewicz, "Discrete-time quasi-sliding-mode control strategies," *IEEE Trans. Ind. Electron.*, vol. 45, no. 1, pp. 633-637, 1998.

- [59] Werner, H., Robust Control of a Laboratory Flight Simulator by Nondynamic Multirate Output Feedback, *Proc. IEEE Conf. Decision and Control*, pp. 1575-1580, 1996.
- [60] S. Janardhanan, B. Bandyopadhyay and T. C. Manjunath, Fast Output Sampling Based Output Feedback Sliding Mode Control Law For Uncertain Systems", *Proc. Third Intl. Conf. on System Identification and Control Problems, SICPRO - 2004*, Moscow, Russia, no. 23010, pp. 1300 - 1312, Jan. 2004.
- [61] T.C. Manjunath, B. Bandyopadhyay and S. Janardhanan, "Multirate Output Feedback based Sliding Mode Controller Design for Active Vibration Control of SISO Smart Structures," *Proc. 29th National Systems Conference (NSC-2005)*, IIT Bombay, Mumbai, India, Paper no. 54, Dec. 2005.
- [62] T.C. Manjunath, B. Bandyopadhyay and S. Janardhanan, "Vibration Control of Smart Structures Using Multirate Output Feedback Sliding Mode Control Law," *Proc. 1st National Conference on Control and Dynamical Systems (NCCDS 05)*, IIT Bombay, Mumbai, India, Paper no. 61, Jan. 2005.
- [63] T.C. Manjunath and B. Bandyopadhyay, "Smart Control of Cantilever Structures Using Output Feedback," *International Journal of Simulation, System Science and Technology*, A Special issue on Modelling, Simulation and Decision Support, vol. 7, nos. 4-5, pp. 51-68, Jul. 2006.
- [64] B. Bandyopadhyay and S. Janardhanan, "Discrete time sliding mode control - A multirate output feedback approach," *Springer Publications., Lecture Notes in Control and Information Sciences*, LNCIS No. 323.

1993. In 1996, he was with the Lehrstuhl für Elektrische Steuerung und Regelung, Ruhr Universität Bochum, Bochum, Germany, as an Alexander von Humboldt Fellow. He revisited the Control Engineering Laboratory of Ruhr University of Bochum during May-July 2000. He has authored and coauthored 7 books and book chapters, 60 national and international journal papers and 125 conference papers. He has given a number of seminars in India and abroad. His research interests include the areas of large-scale systems, model reduction, reactor control, smart structures, periodic output feedback control, fast output feedback control and sliding mode control. Prof. Bandyopadhyay served as Co-Chairman of the International Organization Committee and as Chairman of the Local Arrangements Committee for the IEEE International Conference in Industrial Technology, held in Goa, India, in Jan. 2000. His biography was published in Marquis' Who's Who in the World in 1997. Prof. B. Bandyopadhyay has been nominated as one of the General Chairmen of IEEE ICIT conference to be held in Mumbai, India in December 2006 and sponsored by the IEEE Industrial Electronics Society.



**T. C. Manjunath**, born in Bangalore, Karnataka, India on Feb. 6, 1967 received the B.E. Degree in Electrical Engineering from the University of Bangalore in 1989 in First Class and M.E. in Automation and Control Engineering with specialization in Automation, Control and Robotics from the University of Gujarat in 1995 in First Class with Distinction, respectively. He has got a teaching experience of 17 long years in various engineering colleges all over the country and is currently a Research Scholar doing his Ph.D. in the Department of Systems and Control Engineering, Indian Institute of Technology Bombay, Powai, Mumbai-400076, India, in the field of modeling, simulation, control and implementation of smart flexible structures using DSpace and its applications. He has published 72 papers in the various national, international journals and conferences and published two textbooks on Robotics, one of which has gone upto the third edition and the other, which has gone upto the fourth edition along with the CD which contains about 200 C / C++ programs for simulations on robotics. He is a student member of IEEE since 2002, SPIE student member and IOP student member since 2004, life member of ISSS and a life member of the ISTE, India. He has visited Singapore, Russia, United States of America and Australia for the presentation of his research paper in various international conferences. His biography was published in 23<sup>rd</sup> edition of Marquis' Who's Who in the World in 2006 issue. He has also guided more than 2 dozen robotic projects. His current research interests are in the area of Robotics, Smart Structures, Control systems, Network theory, Mechatronics, Process Control and Instrumentation, CT and DT signals and systems, Signal processing, Periodic output feedback control, Fast output feedback control, Sliding mode control of SISO and multivariable systems and its applications.



**B. Bandyopadhyay**, born in Birbhum village, West Bengal, India, on 23<sup>rd</sup> August 1956 received his Bachelor's degree in Electronics and Communication Engineering from the University of Calcutta, Calcutta, India, and Ph.D. in Electrical Engineering from the Indian Institute of Technology, Delhi, India in 1978 and 1986, respectively. In 1987, he joined the Interdisciplinary Programme in Systems and Control Engineering, Indian Institute of Technology Bombay, India, as a faculty member, where he is currently a Professor. He visited the Center for System Engineering and Applied Mechanics, Universite Catholique de Louvain, Louvain-la-Neuve, Belgium, in